The Role of Host Calcium Signaling in *Toxoplasma gondii* egress

Stephen A. Vella[1,2], Christina A. Moore[1,3], Zhu-Hong Li[1], Miryam A. Hortua Triana[1], Evgeniy Potapenko[1] and Silvia N J Moreno[1,3,*]

From the [1]Center for Tropical and Emerging Global Diseases, [2]Department of Microbiology and [3]Department of Cellular Biology, University of Georgia, Athens, GA, 30602

Running title: *Host calcium and Toxoplasma egress*

[*]Corresponding author: smoreno@uga.edu

Keywords: *Toxoplasma gondii,* calcium signaling, genetically-encoded calcium indicators, GCaMP6f, RGECO, LAR-GECO, jGCaMP7f, Toxoplasma egress

Abstract

Toxoplasma gondii, an obligate intracellular parasite, is capable of invading virtually any nucleated cell. Active invasion by the parasite is a precise process and intracellular parasites reside and replicate inside a parasitophorous vacuole (PV). The membrane of the PV functions as a molecular sieve allowing for its ionic milieu to be in equilibrium with the host cytosol. The parasite would thus be exposed to the ionic fluctuations of the host cytoplasm, such as increases in host cytosolic Ca^{2+} during Ca^{2+} signaling events. Ca^{2+} is a universal signaling molecule and both the host cell and *T. gondii* will utilize Ca^{2+} signaling to stimulate diverse cellular functions. Using *T. gondii* tachyzoites and host cells expressing genetically encoded Ca^{2+} indicators, we demonstrate that host Ca^{2+} signaling impacts intracellular Ca^{2+} levels of the parasite. We propose that Ca^{2+} influx derived from host Ca^{2+} signaling into the parasite is utilized to maintain the intracellular Ca^{2+} stores replenished as the parasite replicates within the low Ca^{2+} environment of the host cell. Intracellular Ca^{2+} store(s) release is needed to reach the initiation spike in Ca^{2+} that meets the threshold of Ca^{2+} needed to initiate the tightly coordinated process of egress. Post activation of the signal and subsequent microneme secretion, would cause breakdown of the host cell and allow for extracellular Ca^{2+} influx, causing a second, larger spike in Ca^{2+} and activation of the glideosome, the main motility machinery. To directly deliver precise concentrations of ions needed for egress, we used patch-clamped infected host cells and monitored parasite egress. In doing so, we discovered an alternative role for K^+ in timing parasite egress. This is the first study using whole-cell patch clamp to study the role of ions such as K^+ and Ca^{2+} in *T. gondii* egress.

Author Summary

Toxoplasma gondii is an intracellular parasite that causes disease by engaging in multiple rounds of a lytic cycle which consists of invasion, replication inside a parasitophorous vacuole (PV) and egress, resulting in lysis of the host cell. In intracellular parasites, the release of Ca^{2+} from intracellular stores forms part of a series of signaling events that culminate in stimulation of motility and egress. This means that intracellular parasites must be able to uptake Ca^{2+} while replicating to keep their intracellular stores filled to be used during egress. This is not an insignificant task considering that they are inside a PV surrounded by the host cytosol which contains Ca^{2+} below 100 nM. We present data showing that the host Ca^{2+} increases are able to

reach the parasite cytosol through a Ca^{2+} influx mechanism sensitive to nifedipine. This influx causes oscillations that are the result of Ca^{2+} increase and re-uptake by intracellular stores. A Ca^{2+} threshold was needed for egress, extracellular Ca^{2+} influx was relevant for egress and potassium had a modulatory effect on egress. We used infected patched host cells, a novel approach that leaves the host cell intact while allowing changes of PV surrounding buffers.

Introduction

The pathogenesis caused by the infection with *Toxoplasma gondii* is linked to the ability of the parasite to engage in multiple rounds of a lytic cycle which consists of invasion of host cells, replication inside a parasitophorous vacuole (PV), and egress resulting in lysis of the host cell, followed by invasion of a new host cell [1, 2]. Several key steps of the lytic cycle of *T. gondii:* egress, invasion, attachment, and motility, are regulated by fluctuations in cytosolic Ca^{2+} concentrations [3, 4].

Ca^{2+} is a universal signaling molecule and plays important roles in the regulation of a large number of cellular functions [5]. The cytosolic concentration of Ca^{2+} is highly regulated, because prolonged high cytosolic Ca^{2+} levels are toxic and may result in cell death. A variety of Ca^{2+} pumps, channels, and transporters, located at the plasma membrane (PM) and to intracellular stores (endoplasmic reticulum (ER), acidic stores and mitochondria) are involved in maintaining cytosolic Ca^{2+} levels under control [5].

In *Toxoplasma* Ca^{2+} signaling initiates a chain of events that leads to the activation of specific effectors involved in the regulation of motility as gliding parasites loaded with fluorescent Ca^{2+} indicators as well as expressing Genetically Encoded Calcium Indicators (GECIs) show Ca^{2+} oscillations [6, 7]. Previous studies have shown that increasing cytoplasmic Ca^{2+} activates the motility machinery leading to egress. Blocking these cytosolic Ca^{2+} fluxes using BAPTA-AM (membrane permeable cytosolic Ca^{2+} chelator), blocks motility, conoid extrusion (apical tip of cell necessary for attachment), invasion, and host cell egress [8].

Active egress of *Toxoplasma* from host cells requires rupture of the parasitophorous vacuole membrane (PVM) and the host cell membrane [9]. Egress is essential for the dissemination of the infection and it has been known for several years that Ca^{2+} ionophores can trigger egress [10]. However, it was the use of GECIs that provided the final and conclusive evidence that there was a cytosolic Ca^{2+} increase right before egress [7]. Secretion of the perforin-like protein 1

(TgPLP1) from micronemes (specialized secretory organelles involved in egress, motility, and invasion by tachyzoites), assists in the permeabilization of the PVM and host cell membrane [11]. Both secretion of the microneme protein TgPLP1 and initiation of motility during egress are stimulated by an increase in cytosolic Ca^{2+}.

As an obligate intracellular parasite, *T. gondii* resides and replicates within the PV that functions as a molecular sieve to passively permit the exchange of small molecules; thus, the surrounding milieu of intracellular parasites is likely in equilibrium with the host cell cytoplasm [12]. Therefore, intracellular parasites are likely exposed to the fluctuations of the host cytosolic ionic composition. The host cytoplasmic Ca^{2+} level is highly controlled and kept at physiological levels of ~70-100 nM under basal conditions, which is similar to the cytoplasmic levels of the replicating parasites. Experimental evidence indicates that Ca^{2+} efflux from intracellular stores represent the first initial step of the Ca^{2+} signaling pathway for egress, so maintaining the high Ca^{2+} levels of the stores is fundamental for continuation of the lytic cycle. The question is how the parasite keeps its intracellular stores replenish while replicating surrounded by such low Ca^{2+} concentration. We hypothesize that the intracellular parasite will uptake Ca^{2+} from the host cytosol during host signaling events. For this to be possible, the parasite would need an efficient and high affinity influx system for Ca^{2+} at its plasma membrane.

There is some evidence for the importance of host cytosolic Ca^{2+} during growth of intracellular parasites, like the inhibitor L-651,582 which blocked Ca^{2+} entry into the host cell and negatively affected parasite replication [13]. It was also proposed that the PV may contain higher concentration of Ca^{2+} [14].

Here, we characterized the role of host cell calcium in parasite egress. Using a variety of pharmacological tools, fluorescence microscopy, and a novel approach using patch-clamped host cells, we show that Ca^{2+} signaling of the host cell impacts parasite Ca^{2+} levels and drives parasite egress. Because previous work showed a key role for K^+ ions we also studied the role of this ion and propose an alternative role for K^+, involved in parasite egress and its link to Ca^{2+} influx.

Results

Parasites are Liable to Host Ca^{2+} Fluxes

We have previously showed that permeabilization of the plasma membrane of infected Hella cells with saponin in the presence of 2 mM extracellular Ca^{2+} induced Ca^{2+} oscillations within parasites that correlated with parasite egress, therefore we reasoned that parasites are susceptible to host cytosolic Ca^{2+} fluxes [7]. We therefore investigated how host cytosolic Ca^{2+} signaling interacted or affected the cytosolic Ca^{2+} levels of intracellular tachyzoites residing within a PV. With this aim, we expressed Ca^{2+} genetic indicators (GECIs) like RGECO or jRGECO1a in the cytoplasm of HeLa cells [15, 16] and infected them with *T. gondii* tachyzoites expressing either cytosolic GCaMP6f or jGCaMP7f [17] targeted to the lumen of the PV (See Material and Methods and Table S1). We grew Hela cells on coverslips, transfected them with the a GECI expressing plasmid and infected these cells with GECI-expressing tachyzoites. To follow Ca^{2+} changes, we used time-lapse microscopy and stimulated the infected cells with specific host cell agonists (Figs 1 and S1). We first used carbachol, a muscarinic receptor agonist that specifically acts on mammalian host cells and stimulates Ca^{2+} oscillations [18]. Muscarinic receptors, stimulated by the neurotransmitter acetylcholine, are well-characterized G-coupled protein receptors that lead to an increase in cytosolic Ca^{2+} via activation of a phosphatidyl inositol phospholipase C (PI-PLC) and generation of inositol 1,4,5-trisphosphate (IP_3) [19]. We observed a dramatic rise in the fluorescence of RGECO or jRGECO1a, indicating an increase in host cytosolic Ca^{2+} (Fig 1A, *red tracings*). For the experiment shown in Fig 1A, the tachyzoites expressed jGCaMP7f in the PV, which was achieved by fusing the *T. gondii* P30 gene to the N-terminus of the GECI, which was shown to confer localization to the PV [11]. We observed an almost simultaneous rise in PV Ca^{2+} after stimulation of host Ca^{2+} with carbachol (Fig 1A, *green tracing*) thereby supporting the molecular sieve model of the PV [12]. Next, we looked at the response of parasite cytosolic Ca^{2+} following host cytosolic Ca^{2+} stimulation. We used HeLa cells expressing a cytosolic copy of RGECO and infected them with tachyzoites expressing GCaMP6f in their cytoplasm. The rise of host cytosolic Ca^{2+} led to stimulation of Ca^{2+} oscillations in the parasites as observed by the increase of green fluorescence of GCaMP6f (Fig 1B, *green tracing* and Supplemental Video 1). We next investigated the link between PV Ca^{2+} and parasite cytosolic Ca^{2+} and for this, we infected HeLa cells with parasites expressing GCaMP6f within their cytosol and a copy of RGECO localized to the lumen of the PV. Carbachol addition caused a uniform rise in all PVs expressing the GECI, followed by a small proportion of parasites showing increase in cytosolic Ca^{2+} (GCaMP6f signal) (Fig 1C). It is possible that this phenotype represents parasites at different

stages of the replication cycle that are more or less sensitive to Ca^{2+} influx. All parasites within the same PV were exposed to the same rise in luminal PV Ca^{2+} as indicated in the fact that all PV's responded to carbachol stimulation (Fig 1A), yet only a few parasites showed a subsequent increase in parasite cytosolic Ca^{2+} (Fig 1B).

We repeated our experiments assessing the Ca^{2+} waves between host-PV-parasite cytosol by stimulating host Ca^{2+} increase using Histamine (Fig S1). Histamine functions through a similar, though different G-coupled protein receptor than carbachol. Histamine will also induce an IP_3 mediated increase in cytosolic Ca^{2+} [20]. The results with histamine were similar to the ones with carbachol in which a rise in host cell Ca^{2+} occurred simultaneous with PV Ca^{2+}. Additionally, parasite Ca^{2+} influx trailed host Ca^{2+}. Taken together these results demonstrate that host Ca^{2+} signaling resulting in cytosolic Ca^{2+} increases can be taken up by intracellular parasites residing inside their PV.

A Threshold of Ca^{2+} is needed for Parasite Egress

With the aim to better visualize the link between host Ca^{2+} signaling and intracellular parasite Ca^{2+} fluctuations and egress, we transiently transfected HeLa cells with LAR-GECO1.2 (a red Ca^{2+} indicator optimized for expression within the host mitochondria) [21] and infected the host cells with cyto-GCaMP6f expressing tachyzoites. We stimulated Ca^{2+} increase with ionomycin, a Ca^{2+}/H^{+} ionophore which causes Ca^{2+} release from all neutral stores into the cytoplasm [22], or thapsigargin (TG), an inhibitor of the endoplasmic reticulum (ER) Ca^{2+}-ATPase SERCA (Fig 2A&B) [23]. The ER constantly allows efflux of Ca^{2+} via an unknown mechanism, and the SERCA serves as a counterbalance to pump Ca^{2+} back into the organelle. Blocking of SERCA via thapsigargin will induce a rise in cytosolic Ca^{2+} due to the ER's constant efflux of Ca^{2+} [23]. The addition of ionomycin leads to a dramatic Ca^{2+} increase in both the host and parasite, followed by rapid egress (Fig 2A&C). Addition of TG induced an increase in the fluorescence of LAR-GECO, indicating an increase of Ca^{2+} within the host mitochondria (LAR-GECO), as well as Ca^{2+} oscillations within the parasite (GCaMP6f). The increase in host mitochondrial Ca^{2+} can be accounted for as due to the close, tight interaction between the ER and the mitochondria [24]. Interestingly, addition of TG caused Ca^{2+} oscillations in the intracellular tachyzoites but they remained intracellular throughout all 10 min of recording (Fig 2B&D and Supplemental Video 2).

We next tested Zaprinast, a cGMP phosphodiesterase inhibitor, which has been shown to stimulate an increase in cytosolic Ca^{2+} and egress [25, 26]. The increase of cytosolic Ca^{2+} by Zaprinast was almost comparable to the increase observed with ionomycin, and also resulted in egress (Fig 2E). However, while both histamine and thapsigargin did induce an increase in parasite cytosolic Ca^{2+}, the response was insufficient to induce egress. We compared the fluorescence tracings for ionomycin and zaprinast to histamine and thapsigargin. Ionomycin and Zaprinast produced a $\Delta F_{max}/F_0$ of approximately 6 that was not statistically different between the two. Thapsigargin and histamines' $\Delta F_{max}/F_0$ response was much lower of approximately ~2 fold that was not statistically different between the two reagents. Comparing Ionomycin to either thapsigargin or histamine and Zaprinast to either thapsigargin or histamine, shows that the responses were statistically different (Fig 2E). Our results suggest that a threshold for cytosolic Ca^{2+} has to be met in order to induce egress.

We next characterized the Ca^{2+} threshold needed for egress and for this we titrated down ionomycin to determine a concentration that would still produce a Ca^{2+} response but was insufficient to induce egress. As expected, the standard concentration of 1 μM ionomycin induced a rapid egress response (Fig 2F&H). As we lowered the concentration of ionomycin down to 0.1 μM and 0.01 μM the ΔFluorescence response decreased as well, though parasite egress was still observed. No egress was observed when the ionomycin concentration was lowered to 0.005 μM (Fig 2G&I). It is significant to note that the ΔFluorescence response of 0.005 μM was approximately 3, a value closely similar to the responses of thapsigargin and histamine that also did not produce a sufficient response to induce egress (Fig 2E&J). The cytosolic Ca^{2+} concentration that tachyzoites reached in response to various concentrations of Ionomycin were evaluated in a separate experiment with extracellular tachyzoites loaded with the ratiometric Ca^{2+} indicator Fura-2-AM (Fig S3). The cytosolic concentration reached for Ionomycin at 5 nM was ~250 nM and at 10 nM IO was around 750 nM. Therefore, from these experiments we could conclude that there a cytosolic Ca^{2+} threshold that needs to be reached for the stimulation of egress and it is around 300-500 nM.

Two Peaks of Ca^{2+} Lead to Parasite Egress

We wanted to examine if intracellular parasites are able to influx Ca^{2+} and if this influx impacts parasite egress. We first examined parasite cytosolic Ca^{2+} fluctuations when artificially exposed

to the extracellular buffer by permeabilizing the host plasma membrane with saponin (Fig 3). We tested two conditions: Ca^{2+} free (100 μM) and Ca^{2+} rich (2 mM Ca^{2+}) buffers. When parasites were exposed to Ca^{2+} free extracellular buffer, they did not egress, though a sharp single peak was evident after quantifying the fluorescence tracings (Fig 3A-B). In comparison, when using a Ca^{2+} rich buffer after permeabilizing the host membrane to expose the parasites to the extracellular buffer, cytosolic Ca^{2+} levels oscillated and they promptly egressed from their respective PV's (Fig 3C-D). These results demonstrated that intracellular parasites uptake Ca^{2+} and this influx can trigger egress.

We next stimulated egress with Zaprinast, which inhibits a cGMP phosphodiesterase resulting in a build-up of cGMP that activates protein kinase G (PKG) and leads to a cytosolic Ca^{2+} increase by an unknown mechanism. This Ca^{2+} increase results in stimulation of microneme secretion, and parasite egress. We performed the egress experiment in an extracellular buffer supplemented with 2 mM Ca^{2+} and noticed that egressing parasites displayed a quantifiable, characteristic two fluorescence peaks that preceded egress (Fig 3E-G and Supplemental Video 3). We repeated the Zaprinast induced egress experiments with extracellular buffer supplemented with 100 μM EGTA (Ca^{2+} free) and quantified the response. Under these conditions the second peak was lower, and the fluorescence peak wider (Fig 3H-J). Parasites took longer to egress when Zaprinast was added in Ca^{2+} free buffer compared to egress in extracellular buffer supplemented with 2 mM Ca^{2+} (Fig 3J).

Of interest is the microneme protein, Perforin-Like Protein 1 (PLP1), which functions in breaking down the host cell during egress, exposing intracellular tachyzoites to the surrounding extracellular milieu. PLP1 has been shown to be involved in the initial rupture of the PV [11] and the release of Ca^{2+} from intracellular stores could stimulate this release in the natural egress process. Our model proposes that this rupture would allow the extracellular Ca^{2+} to influx the parasites contributing to reaching the threshold for downstream stimulation of gliding motility and egress. We next tested whether ΔPLP1 mutants, defective in their ability to breakdown the host cell, would still display two peaks during egress. Under this hypothesis ΔPLP1 mutants would have altered Ca^{2+} fluorescence tracings of the second peak due to ineffectively PVM breakdown to enable Ca^{2+} entry. We transfected GCaMP6f into ΔPLP1 mutants and induced egress using 100 μM Zaprinast (Fig S2). We quantified the fluorescence tracings of egressing parasites and these

cells only displayed 1 peak (Fig S2B &C) supporting that the second peak is due to influx from the extracellular milieu.

A Ca^{2+} Peak Precedes Natural Egress from Host Cells

Our previous model predicts that a rise in intracellular Ca^{2+} originating from intracellular stores, further enhanced with extracellular Ca^{2+} influx drives natural egress [7]. To observe how Ca^{2+} levels fluctuate during natural egress we synchronized intracellular parasites using compound 1 (cpd1) (Fig 4 and Supplemental Video 4). In the related Apicomplexa parasite *Plasmodium falciparum,* cpd1 reversibly inhibits PKG and arrests parasites from egressing [27]. After washing off the drug, merozoites egressed rapidly from red blood [27]. We applied this approach to *T. gondii* in the hopes to visualize natural egress. GCaMP6f expressing parasites were allowed to infect stably expressing jRGECO1a HeLa cells and were synchronized 24 hr post infection with cpd1. Within two minutes after cpd1 washout parasite cytosolic Ca^{2+} increased. The increase was nonuniform within a given PV and instead began with a single "leader" tachyzoite that was distinguishable due to having the initial largest increase in cytosolic Ca^{2+} that preceded all other tachyzoites, and this cell egressed first (Fig 4 A). We quantified the fluorescence tracings, and as expected, egressing parasites displayed two peaks during egress (Fig 4 C-E). Interestingly, a rise in host Ca^{2+} was also evident during the natural egress process, thus highlighting the role of extracellular Ca^{2+} influx during natural egress (Fig. 4C&D, *red tracing*). Next we tested how ΔPLP1 parasites would respond under natural egress conditions (Fig. 4B&F). Post cp1 washout, ΔPLP1 GCaMP6f oscillated randomly and nonuniformly, and no parasite exhibited the two-peak pattern we witnessed in wild type parasites (Fig. 4F). Characteristic to ΔPLP mutants, some parasites displayed movement within their PV [11] post rise in cytosolic Ca^{2+} though none of these parasites displayed a second peak of higher amplitude that would be associated with Ca^{2+} influx, as well as no rise in the jRGECO1a channel that would be indicative of rupture of the host cell and extracellular Ca^{2+} influx. Eventually the fluorescence of these parasites diminished indicating lower cytosolic Ca^{2+}, and the parasites stopped moving shortly after. Given these results, we conclude that two-peaks of Ca^{2+} are evident under a natural egress of *T. gondii*.

Blocking Ca^{2+} Influx Using Pharmacological Agents Blocks Parasite Egress

Previously, we showed that Ca^{2+} influx occurs through a nifedipine sensitive channel [7, 28]. We next wondered whether pharmacologically blocking Ca^{2+} influx would affect the two peaks that we observed during parasite egress. We pretreated intracellular cyto-GCaMP6f-expressing parasites with 10 μM nifedipine for comparison with non-treated parasites in egress experiments. We exposed the parasites to the surrounding extracellular buffer supplemented with 2 mM Ca^{2+} using saponin. As expected, the non-treated parasites egressed following a sharp rise in cytosolic Ca^{2+} trailed by smaller Ca^{2+} oscillations (Fig 5A &B). We compared this phenotype to nifedipine pretreated parasites. Even after saponin treatment and exposure to Ca^{2+} rich extracellular buffer, parasites did not egress, and only modest Ca^{2+} oscillations of approximately two-fold range were evident (Fig 5C&D), which are below the threshold needed for egress (Fig 2). We next tested whether blocking PKG with cpd1 would alter the two peaks needed for egress. We induced egress using Zaprinast in control parasites and cpd1-pretreated parasites expressing GCaMp6f. While control parasites egressed following a fast rise in cytosolic Ca^{2+} with two peaks (Fig 5E&F) pretreatment with cpd1 abolished egress, and the parasites' cytosolic Ca^{2+} only raised about 3-fold (Fig 5G&H). These results showed that blocking extracellular Ca^{2+} influx with nifedipine or inhibiting PKG, results in intracellular parasites that are unable to reach the threshold needed for egress, in support for the role of extracellular Ca^{2+} influx in egress.

Role of K^+ and Ca^{2+} in parasite egress

The cytosol of eukaryotic cells contains approximately 140 mM K^+ with 70-90 nM Ca^{2+}, while the extracellular milieu contains 5 mM K^+ and ~1.8 mM Ca^{2+}. During a Ca^{2+} signaling event, cytosolic Ca^{2+} rises rapidly to μM levels [5], and we have shown that a crosstalk exists between the host cell and the parasite cytosolic Ca^{2+} (Fig 1). To manipulate the host cytosolic ionic composition, and identify the Ca^{2+} concentration that would induce parasite egress, we used whole-cell patch clamping of infected HeLa cells [29]. We attached a pipet to the plasma membrane of infected cells as shown in Fig 6A, formed a patch seal between the plasma membrane and the patch pipette, and broke the plasma membrane, thus equilibrating the solution in the patch pipette with the cytosol of the host cell. This technique allowed us to control the composition of the buffer surrounding the PVs by modifying the pipet buffer (Fig 6A). We tested increasing concentrations of cytosolic free Ca^{2+} (0.5, 1, 5, and 10 μM) in a 140 mM K^+ patch pipette solution (Fig. 6B). We did not observe egress at 0.5 μM Ca^{2+}, and only a small percentage of parasites egressed at 1 μM

Ca^{2+}. Approximately one third of parasites egressed when exposed to 5 μM Ca^{2+} while the remaining two thirds did not egress. Ultimately at a concentration of 10 μM Ca^{2+}, all parasites egressed (Supplemental Video 5). Previous literature has stated that the high potassium environment of the host cytosol creates an inhibitory effect that prevents parasite egress. It was postulated that a decrease in the concentration of potassium would activate a Ca^{2+} signal, inducing microneme secretion and subsequent egress [30]. To test the role of potassium in parasite egress, we repeated the whole-cell patch clamp experiments in a low potassium solution within the patch pipette (Fig 6C). Choline chloride was added to maintain the same osmolarity and anionic composition. We first whole-cell patch clamped cells at a low concentration of potassium and low Ca^{2+}, and no egress was observed (data not shown). Under low potassium, we did not observe egress at 0.5 μM Ca^{2+} and at 1 μM Ca^{2+}, two thirds of the patched cells egressed, and the parasites egressed faster compared to the high potassium counterpart. Approximately 80% of patched cells egressed at 5 μM Ca^{2+}, and egress occurred in approximately 3 min compared to 5 min in a high potassium solution. Similar to the high potassium conditions, 10 μM Ca^{2+} under low potassium conditions caused 100% egress, but again at a much faster rate. We summarized our patch clamp data in Fig. 6D&E. No egress was observed under both conditions for 0.5 μM Ca^{2+}, but 1 μM Ca^{2+} was sufficient to induce egress, though the percentage and rate of egressing parasites was higher and faster under low potassium conditions. As we increased the cytosolic Ca^{2+} concentration to 2, 5, and eventually to 10 μM Ca^{2+}, the percentage of egressing parasites increased quasi-linearly under the low potassium conditions. Under high potassium conditions the percentage of egressing parasites increased quasi-linearly from 1-5 μM Ca^{2+}, but 10 μM Ca^{2+} was sufficient to induce 100% egress (Supplemental Video 6). Egress was faster under all concentrations in low-potassium conditions. At 1 μM Ca^{2+}, parasites egressed in approximately 550 and 320 sec for high and low potassium, respectively. In high potassium conditions, parasites egressed at about the same rate for 2 and 5 μM Ca^{2+}, but under low potassium conditions parasites egressed faster at 5 μM Ca^{2+} versus 2 μM Ca^{2+} (~300 seconds (2 μM Ca^{2+}) versus ~200 seconds (5 μM Ca^{2+})). Though 100% egress was observed at 10 μM Ca^{2+} for both conditions, in high potassium parasites egressed in ~250 seconds, versus ~50 seconds in low potassium conditions. In summary, according to these results Ca^{2+} is crucial for egress but a decrease in the concentration of K^{+} as the parasite lyses the host cell and egresses, results in acceleration of egress.

Discussion

T. gondii is an obligate intracellular pathogen and replicates inside a highly modified and adapted PV. Egress from the host cell is an essential step for the infection cycle of *T. gondii*. During egress, parasites will leave a likely dying and exhausted host cell and will search for a new one to invade and start a new lytic cycle [31]. It was shown that parasites growing *in vitro* in tissue cultures responded to the addition of ionophores by promptly egressing [10]. It was assumed that Ca^{2+} oscillations were the trigger, and this hypothesis was finally validated by our observations using GECIs allowing for the specific detection of Ca^{2+} changes in intracellular parasites [7]. One of the most important and significant questions that remained is how do intracellular parasites keep their Ca^{2+} stores replenished while replicating inside the host cell, surrounded by the low, physiological (~100 nM) Ca^{2+} levels of the host cytosol. It was also not understood how intracellular and extracellular sources of Ca^{2+} interact/converge to deliver the threshold needed for stimulation of motility and egress. In this work we demonstrated that intracellular parasites are able to take up Ca^{2+} from the host cell during host Ca^{2+} signaling events resulting in cytosolic increases of Ca^{2+} and stimulation of oscillations in the parasite. The PV coupled host-derived Ca^{2+} and Ca^{2+} oscillations in the parasite cytosol. We stimulated Ca^{2+} signaling in infected HeLa cells with natural agonists like carbachol or histamine and followed the Ca^{2+} signals by expressing genetically encoded Ca^{2+} indicators in the parasite, the host cytosol and the parasite PV. A concurrent Ca^{2+} spike was evident in the GECIs expressed within the host cytosol and PV, showing that the PV is permeable to, at least, small molecules [12]. Parasite Ca^{2+} rose following the rise of the host cytoplasmic and PV Ca^{2+}. We observed that a specific Ca^{2+} threshold in the parasite cytosolic Ca^{2+} was required for egress, and we also saw the occurrence of two peaks of cytosolic Ca^{2+} increase, the second one impacted by influx of Ca^{2+} after the rupture of the host cell, as ΔPLP1 mutants, defective in egress, did not exhibit these two peaks. We also observed that reducing the concentration of potassium during egress modulated the rate and timing of egress, though Ca^{2+} influx was sufficient to stimulate egress.

The *T. gondii*'s endoplasmic reticulum expresses a SERCA-type Ca^{2+}-ATPase (TgSERCA) [32]. SERCA-type Ca^{2+}-ATPases pump Ca^{2+} into the ER, thus maintaining the cytosolic concentration low (~70-100 nM) at the expense of high ER Ca^{2+} levels (~μM to mM levels) [5]. While *T. gondii* is inside its host cell is challenged by having to maintain its intracellular stores filled with Ca^{2+} while replicating within the low Ca^{2+} environment of the

mammalian cytosol. Considering that egress can occur at nearly any stage of intracellular replication and is preceded by a spike in cytosolic Ca^{2+} [7], that very likely is initiated by intracellular store release, it is essential that a mechanism to maintain the parasite Ca^{2+} stores continuously replenished is in place so they would be readily released upon the signaling event preceding egress [7].

Carbachol and Histamine both stimulate mammalian cytosolic Ca^{2+}, via signaling pathways involving the production of IP_3, the Ca^{2+} mobilizing second messenger that acts by gating the IP_3 receptor localized to the ER, allowing Ca^{2+} release into the cytosol [33]. Decrease of ER Ca^{2+} leads to the activation of the Store Operated Ca^{2+} Entry (SOCE) pathway, which will contribute to the Ca^{2+} signal by allowing influx through the plasma membrane [34]. In our experimental set-up, stimulation of Ca^{2+} signaling with known mammalian agonists resulted in cytosolic Ca^{2+} increase of ~1-2 μM (higher concentrations would be toxic). Interestingly, we saw that these low levels of Ca^{2+} are sufficient to stimulate Ca^{2+} influx into intracellular parasites followed by Ca^{2+} oscillations. Cytosolic Ca^{2+} oscillations in *T. gondii* tachyzoites were previously observed [6, 32], a fascinating phenomenon for which we do not have a molecular explanation. It is generally believed that Ca^{2+} oscillations arise from cyclical release and re-uptake of intracellularly stored Ca^{2+} [35], and a role for influx through plasma membrane channels has also been demonstrated to be important for the maintenance and delivery of Ca^{2+} into the cytosol. Because of the apparent digital nature of these Ca^{2+} oscillations [36] they would be perfectly suited for signaling specific biological responses like secretion of micronemes, stimulation of motility and egress. It was shown that Ca^{2+} oscillations in extracellular tachyzoites loaded with Ca^{2+} dyes were associated with microneme discharge and bursts of motility [6]. Changes of the Ca^{2+} oscillation patterns by pharmacological agents affected microneme secretion and motility [32, 37] highlighting the role Ca^{2+} oscillations in coordinating lytic cycle progression. In the case of the intracellular tachyzoite, we believe that the Ca^{2+} oscillations, while being insufficient to stimulate egress they serve to ensure the filling of intracellular stores. These oscillations are the result of Ca^{2+} release from the ER through an unknown channel, likely gated by IP_3 [38] followed by re-uptake likely through the SERCA-Ca^{2+} ATPase [32] or the plasma membrane Ca^{2+} pump [39]. The initial increase of cytosolic Ca^{2+} would be the result of uptake from the host through a plasma membrane mechanism and this initial Ca^{2+} increase would stimulate the activity of the PI-PLC at the plasma membrane [40, 41] to synthesize IP_3, which would open the ER channel and release

Ca^{2+} into the cytosol potentiating the Ca^{2+} signals. However, cytosolic Ca^{2+} levels of the parasite are highly buffered [42] and the rising in cytosolic Ca^{2+} will be countered by mechanisms such as the PMCA-ATPase or the SERCA-Ca^{2+}-ATPase to bring the cytosolic Ca^{2+} back to normal levels [8]. Another possible scenario would be that interaction between the plasma membrane Ca^{2+} channel with the ER Receptor, plus Ca^{2+} itself (and other ions and signaling molecules) would result in its opening, a phenomenon similar to what happens in muscle cells, where the Ryanodine Receptor is directly or indirectly modulated by the L-type Ca^{2+} channel, CaV1.1/1.2, Ca^{2+} itself, other ions and small molecules and proteins [43]. Amplification of the initial Ca^{2+} signal occurs through activation of the RyR leading to Ca^{2+} release from the sarcoplasmic reticulum [5]. This second scenario would require close proximity between the ER membrane and the plasma membrane because of the known poor diffusibility of Ca^{2+} in the cytoplasm of cells [44].

The pattern of the Ca^{2+} signals after the addition of Zaprinast or ionomycin was different with higher amplitude of the signals, which rapidly increased and with less oscillations. The amplitude of the cytosolic Ca^{2+} signal could explain the prompt stimulation of egress by both agents. Ionomycin, an ionophore that releases Ca^{2+} from neutral stores stimulated egress at concentrations greater than 5 nM. Zaprinast, an inhibitor of cGMP-selective phosphodiesterases [45] would result in accumulation of cGMP, which will activate Protein Kinase G (PKG), a protein that plays a pivotal role in microneme secretion and tachyzoite egress [26, 46, 47], and results in the stimulation of cytosolic Ca^{2+} and egress by presumably promoting the formation of phospholipase C substrates [48].

Within host cells parasites are stationary, non-motile, and surrounded by low Ca^{2+}, yet activation by an intrinsic signal like phosphatidic acid as recently proposed [49], would start a signaling cascade leading to a rise in cytosolic Ca^{2+} followed by stimulation of motility. Apicomplexan motility functions through a conserved, actomyosin motor that forms a complex termed the glideosome, the main molecular machinery involved in parasite motility, egress, and invasion [9]. Within the glideosome, Regulatory Light Chains (MLC1), Essential Light Chains 1 and 2 (ELC1 and ELC2), Ca^{2+} binding proteins, interact either directly with Ca^{2+} or via Ca^{2+} dependent phosphorylation events to stimulate motility [50]. The binding affinity of ELC is 37 μM [50], a concentration that would only be physiologically possible to reach if we accept/consider the presence of Ca^{2+} microdomains (confined regions of elevated Ca^{2+} at the site of activated/open channels) at the periphery of the parasite likely formed close to plasma membrane Ca^{2+} channels.

This scenario supports the importance of Ca^{2+} influx for the stimulation of motility and egress, necessary to activate the glideosome while the overall cytosolic Ca^{2+} concentration would be maintained low.

The PV of intracellular replicating tachyzoites is encircled by a PV membrane that associates with host cell ER and mitochondria [51]. The ER and mitochondria of mammalian cells play significant roles in Ca^{2+} homeostasis and signaling, and it could be hypothesized that the organelle's presence at the PV membrane may serve a role in the parasite's Ca^{2+} signaling [5]. For example, in pancreatic acinar cells mitochondria serve as a protective "firewall" that functions to confine Ca^{2+} signals to the secretory pole of the cell [52]. Perhaps the association with the host mitochondria may function to protect parasites from prolonged and repetitive host cell Ca^{2+} signaling that would risk induction of premature egress, though it should be noted that not all strains exhibit host mitochondria PV association [53].

In the experiments where we saw egress (Zaprinast, Ionomycin, Saponin with Ca^{2+}, natural egress) we observed two prominent peaks of cytosolic Ca^{2} in the parasites, which were only evident in media supplemented with Ca^{2+}. The second peak was larger and wider, and we attributed it to extracellular Ca^{2+} influx. Extracellular Ca^{2+} influx would flood in as the host cell is lysed and would further increase the amplitude of Ca^{2+} oscillations [7, 28]. Excluding Ca^{2+} from the media, resulted in a muted second peak with parasites taking longer to egress. The first peak of Ca^{2+}, would stimulate microneme secretion and release of PLP1, which would lyse the host cell, exposing the parasite to the high Ca^{2+} milieu of the extracellular buffer, which would promptly stimulate egress. Two results validated this proposal, one was when we observe a singly peak of Ca^{2+} during egress of the parasite mutants of the microneme protein PLP1 (ΔPLP1), which are defective in their ability to breakdown host cells and as a consequence would not permit Ca^{2+} influx thereby moderating the second peak. We also observed one peak when we block Ca^{2+} influx with nifedipine, a Voltage Gated Ca^{2+} channel inhibitor that we previously showed to block Ca^{2+} influx [28]. We are presently trying to determine the molecular nature of this channel.

During natural egress experiments, parasite Ca^{2+} increased and egress did not occur uniformly and instead, a "leader" parasite was observed that began egress from a single PV and would be distinguishable from its other sister parasites, due to it showing the largest, initial fluorescence increase. We think that this leader parasite would be the initial contributor for microneme secretion, in particular PLP1 [11]. Subsequent extracellular Ca^{2+} influx would induce

microneme secretion followed by egress of the tailing parasites. Interestingly, we also observed a Ca^{2+} increase within the host cell cytosol that matched the fluorescence peaks of the parasite and we attribute this peak to the initial influx of Ca^{2+} from the leader parasite's microneme secretion that permeabilizes the host cell leading to Ca^{2+} influx. The second peak would be the subsequent sister parasites egressing due to release of additional PLP1 and further lyses of the host cell and eventual loss of the GECI signal due to its dilution.

The novel approach of patching infected host cells permitted the manipulation of the ionic composition of the host cytosol surrounding the PV, allowing for the control of the concentration of Ca^{2+} and K^+ at defined values while keeping the host cell intact. Low Ca^{2+} (~90 nM) and high K^+ (140 mM K^+) concentrations mirrored the physiological cytosolic concentrations for these ions in the host cytosol. The concentration of K^+ was reduced to 5 mM to mirror the extracellular concentration of this ion. Under both K^+ conditions a threshold was obtained for the concentration of Ca^{2+} outside the PV. There was no egress at low Ca^{2+} concentrations below 500 nM at both concentrations of K^+ while 100% egress was observed at 10 μM Ca^{2+} even overriding the inhibition of the high concentration of K^+. Lowering the concentration of K^+ accelerated egress at all Ca^{2+} concentrations occurring almost explosively at 10 μM Ca^{2+} with egressing parasites being highly motile seeking another host cell to invade. At intermediate concentrations of Ca^{2+}, like 1 and 0.5 μM Ca^{2+}, we observed partial or no egress respectively, in both high or low K^+, with intracellular parasites partially active and motile within the host cell. We attribute this partial egress phenotype to partial release of microneme proteins in the early stages of egress, in which the Ca^{2+} signal is not strong enough to induce complete secretion of enough microneme proteins that would allow for the breakdown of the host cell and exchange of buffer with the extracellular media (and thus additional Ca^{2+} influx). It has been proposed that the high K^+ content of the host cytosol blocked parasite egress [30]. When the integrity of the host cell becomes compromised, the K^+ concentration drops due to diffusion into the extracellular media. This drop in the concentration of K^+ would induce a Ca^{2+} signal that would stimulate parasite egress through activation of a PI-PLC, though the molecules involved in this model are still unknown [30, 41]. PI-PLCs of the delta type, like the type present in *T. gondii* [40] are highly sensitive to Ca^{2+} concentrations and are active at the Ca^{2+} levels present in the cytoplasm of cells [54]. There is no direct connection between PI-PLC activity and K^+ concentration but two genes in the *T. gondii* database (TGME49_238995 and TGME49_273380) are predicted to act as Ca^{2+}-activated K^+ channels. During intracellular growth,

these channels could activate/open in response to Ca^{2+} release from intracellular stores. Initially, no conductance would occur because the potassium concentration of both parasite and host cytosol would be similar. Lysis of the host cell would result in decrease of the concentration of K^+, generating a gradient, and conductance of the ion with loss of K+ from the parasite, leading to an unbalance in the intracellular concentration of K^+ that would be counteracted by a plasma membrane mechanism such as a potassium/proton exchanger that would exchange K^+ for H^+ leading to acidification of the PV, which has been shown to lead to egress [55]. Toxoplasma expresses four predicted sodium proton exchangers and one of them was localized to the plasma membrane of *T. gondii (TgNHE1)* (TGME49_259200) [56], and a second one (TGME49_263480) is predicted to be at the plasma membrane according to ToxoDB LOPIT [57]. It is possible that one of these exchangers could use K^+ instead of Na^+ and be responsible for the exchange activity. According to this potential scenario, Ca^{2+} would be the main trigger and K^+ would have a modulatory role as we observed with the patch egress experiments.

In summary, we propose that as the parasites grow and replicate, host Ca^{2+} derived from Ca^{2+} signaling is taken up by parasites through their plasma membrane and pumped into intracellular stores in order to keep them filled during repetitive rounds of replication (Fig. 7). Egress initiates via an unknown signal that induces release of Ca^{2+} from intracellular stores. Within the PV a leader parasite would respond first with the initial largest Ca^{2+} increase, which would reach the threshold needed for motility induction and secretion of microneme proteins. Release of PLP1 among other microneme proteins would contribute to the partial breakdown of the host cell [11]. This allows for extracellular Ca^{2+} influx and a drop of host K^+, two factors that would both contribute to the egress of the remaining parasites. The cycle would continue in the remaining parasites: a Ca^{2+} spike would occur to reach the threshold for secretion of microneme proteins, complete breakdown of the PV membrane and host cell, and a second and more pronounced peak in Ca^{2+}, culminating in egress of the entire PV of parasites. We found that the decrease in the concentration of K^+ plays a role in timing parasite egress, and calcium influx from the host cell or the extracellular milieu would be essential for parasite egress. The data from this work contributes to our knowledge of host-parasite interaction of *T. gondii* and aids in our understanding of the signaling responses that govern parasite egress. The use of whole-cell patch clamp presents a novel methodology to study the role of ions involved in parasite egress, an essential component of the lytic cycle.

Materials and Methods

Cell Culture

T. gondii tachyzoites (RH strain) were maintained in hTERT human fibroblasts (BD Biosciences) using Dulbeco's modified essential media (DMEM) with 1% fetal bovine serum (FBS), as described previously [58]. GCaMP6f- transfected tachyzoites were maintained under similar conditions, in the presence of 20 μM chloramphenicol. The selection-less strain of GCaMP6f was maintained without drug pressure. hTERT cells were maintained in high glucose DMEM with 10% fetal calf serum (FCS). HeLa cells (ATCC) were used for egress and whole-cell patch clamp experiments and were maintained in DMEM supplemented with 10% FBS, 1 mM sodium pyruvate, and 2 mM L-glutamine. Cell cultures were grown at 37°C with 5% CO_2. Parasites were purified by centrifugation and filtration through a Whatman 8 μM nuclepore membrane (GE Healthcare) followed by a second filtration step through a 5 μM nuclepore membrane. Filtered parasites were counted and centrifuged following the protocols for each experiment.

Chemicals and Reagents

Transient transfections were performed using PolyJet that was purchased from SignaGen (http://signagen.com/). Plasmids for GCaMP6f (fast version of GCaMP6), R-GECO1.2, jGCaMP7f, and LAR-GECO1.2 were obtained from Addgene, and the plasmids were used for transient transfection in HeLa cells. The respective genes were cloned into the *T. gondii* expression vector pCTH3 and pDHFRTubGFP for chloramphenicol and selection-less stable expression of GCaMP6f in tachyzoites, respectively. Thapsigargin, ionomycin, saponin, dithiothreitol (DTT), histamine, Zaprinast, and all other chemicals were obtained from Sigma.

Preparation of GECI-expressing Tachyzoites and HeLa Cells

GCaMP6f expressing parasites were obtained as described previously [7]. Briefly, plasmids for expressing GCaMP6f in *T. gondii* were a gift from Kevin Brown and David Sibley. The coding DNA sequence for GCaMP6f was amplified by PCR and cloned into a *T. gondii* vector for expression downstream the tubulin promoter (pCTH3 and pDTGCaMP6f), using the BglII and AvrII restriction sites and adding a stop codon in front of the GFP sequence. The primers used were forward 5′-AGGCGTGTACGGTGGGAGGTC-3′ and reverse 5′CTTCCTAGGTTACTTCGCTGTCATCATTTG-3′ (Table S1). The Plasmids were

electroporated into the RH strain parasites and clones were selected by chloramphenicol resistance. We then isolated cells with low fluorescence by cell sorting to eliminate those highly fluorescent cells in which the GCaMP6f could be buffering Ca^{2+} and preventing visualization of physiological changes in Ca^{2+} levels [59].

HeLa cells (5 x 10^5) were grown on coverslips in high-glucose DMEM with 10% FBS. After 24 hours, cells were transfected with 1 µg of plasmid DNA encoding RGECO or LAR-GECO1.2 using PolyJet following the instructions of the manufacturer. 6-8 hours later, HeLa cells were infected with 1 x 10^6 tachyzoites expressing GCaMP6f and were grown for 15-20 hours. Rosettes containing 4-8 parasites were used in all experiments. To construct a cell line of Hela cells stabling expressing the sensitive red GECI, jRGECO1a, the coding sequence of jRGECO1a [15] was PCR amplified with primers Fwd 5'- ACCGGTATGCTGCAGAACGAGCTTGCTCTTA -3' and Rev 5' -GAATTCGCCTACTTCGCTGTCATCATTTGTACA-3' and cloned into the TOPO vector sequence. The resulting product was digested with AgeI and EcoRI restriction enzymes and cloned into the 2nd generation lentivirus expression plasmid pUltra (Table S1). Transfection and cloning of a stable cell line of jRGECO1a was performed using previously established protocols [60]. Briefly, 2nd generation viral particles were produced in HEK293T cells, and the viral supernatant was overlaid on Hela cells for spinfection for 2 hr. Stable cell lines were enriched and selected using FAC's sorting.

Cytosolic Ca^{2+} Measurements

Extracellular tachyzoites of the RH strain were loaded with fura-2-AM as described previously [28]. The parasites were washed twice in Ringer buffer (155 mM NaCl, 3 mM KCL, 2 mM $CaCl_2$, 1 mM $MgCl_2$, 3 mM NaH_2PO_4, 10 mM Hepes, pH 7.3, and 5 mM glucose), resuspended in the same buffer to a final density of 1 x 10^9 cells/mL, and kept on ice. For fluorescence measurements, 50 µL-portions of the cell suspension were diluted in 2.5 mL of Ringer (2 x 10^7 cells/mL final density) in a cuvette placed in a thermostatically controlled Hitachi 4500 spectrofluorometer. Excitation was at 485 nm and emission at 520 nm. Traces shown are representative of three independent experiments conducted on separate cell preparations. Calcium-defined conditions were determined by using EGTA or 1,2-bis(2-aminophenoxy)ethane-*N*,*N*,*N′*,*N′*-tetraacetic acid (BAPTA) and calcium chloride to reach specific concentrations of free calcium. Calcium-EGTA

combinations were determined using Maxchelator software (https://somapp.ucdmc.ucdavis.edu/pharmacology/bers/maxchelator/downloads.htm).

Egress Assays

Egress assays were done as described previously [59]. HeLa cells were grown in high glucose DMEM with 10% FBS in 35 mm glass bottom dishes (MatTek) until confluency. 8-12 hours after transfection, HeLa cells were infected with 1 x 10^6 GCaMP6f-expressing tachyzoites, replacing the media with high glucose DMEM with 1% FBS. Thirty hours after infection, parasitophorous vacuoles containing 4-8 parasites were observed by microscopy after washing them in the specific buffer for each experiment. Drugs were added 1 minute after the start of imaging in that same buffer at the concentrations indicated: ionomycin (0.005-1 μM), histamine (100 μM), thapsigargin (1 μM), saponin (0.01%), nifedipine (10 μM), and zaprinast (100 μM). Ringer buffer was used as extracellular buffer (EB). $CaCl_2$ was omitted in the absence of extracellular calcium, and the media was supplemented with either 100 μM EGTA, 1 mM EGTA or 1 mM BAPTA. The composition of intracellular buffer (IB) is: 140 mM potassium gluconate, 10 mM NaCl, 2.7 mM $MgSO_4$, 2 mM ATP (sodium salt), 1 mM glucose, 200 μM EGTA, 65 μM $CaCl_2$ (90 nM free Ca^{2+}), and 10 mM Tris/Hepes, pH 7.3. The parasites were imaged at 37°C. Fluorescence images were captured using an Olympus IX-71 inverted fluorescence microscope with a Photometrix CoolSnapHQ charge-coupled device (CCD) camera driven by DeltaVision software (Applied Precision). Images were collected using time-lapse mode with an acquisition rate of at least 2-3 seconds during 10-20 minutes. Images were converted into videos using SoftWorx suite 2.0 software from Applied Precision. Fiji was used for the analysis of the video data. Fluorescence tracings were produced by drawing an ROI around the host or parasite of interest and measuring the mean gray fluorescence. Prism was used for statistical analysis.

For natural egress, 3.5 x 10^5 Hela cells stabling expressing the red GECI jRGECO1a [15] were plated on 35 mm glass bottom MatTek dishes in DMEM-HG with 10% FBS. 24 h later cells were infected with 2.75 x 10^6 parasites, and on day three the parasites were synchronized using 1 μM compound, and one dish was treated with 2 μL of DMSO as a vehicle control. On day four lysis of the control dish was examined for 70-80% lysis, and the synchronized dishes were used for video microscopy. The dishes were washed once with pre-warmed Ringer buffer, then again with

pre-warmed Ringer buffer for 1 minute and finally a solution of Ringer buffer supplemented with 2 mM $CaCl_2$ was added before commencing imaging.

Whole cell patch clamping

Whole cell patch clamp recording was applied according to the method previously described [61, 62]. Briefly, coverslips with infected HeLa cells were transferred into a perfusion chamber (RC-26GLP, Warner Instruments, USA) on a stage of an inverted IX51 Olympus microscope. Growth media was immediately replaced with an extracellular buffer prior to the start of the recordings, and cells were kept at room temperature for no more than 2 hours. Coverslips were replaced every 2 hours. Intracellular thin-walled recording capillars (1.5-mm outer diameter, 1.17-mm inner diameter) made of borosilicate glass (World Precision Instruments, Sarasota, FL) were used to pull patch pipettes (3–4 MΩ) on a horizontal Flaming/Brown micropipette puller (P-97, Sutter Instruments) and then were backfilled with intracellular solution. Recordings from HeLa cells were obtained with an Axopatch 200B amplifier (Molecular Devices) using high-resolution videomicroscopy (Ameriscope). The voltage output was digitized at 16-bit resolution, 20 kHz, and filtered at 1 kHz (Digidata 1550A, Molecular Devices). All experiments were performed at -60 mV holding membrane potential (Vh) which is close to values reported as physiological for HeLa cells [63] to prevent activation of voltage-gated calcium channels. After establishing a "seal" (>1 MΩ) slight negative pressure was applied together with "ZAP" electrical pulse (0.5-5 ms, +1.3V) to break cell membrane. The time from membrane opening (start of pipette/cytosol solution exchange) to egress was visually recorded. All statistical analyses were conducted using GraphPad Prism 5 (GraphPad Software, San Diego, CA). All values are expressed as means ± SE. Between-group differences were compared using unpaired *t*-tests. Differences were considered statistically significant at $P < 0.05$, and *n* refers to the number of cells.

HeLa cells grown in high glucose DMEM with 10% FBS on 22 x 40 mm glass coverslips until 70% confluency were infected with 1 x 10^6 GCaMP6f-expressing tachyzoites. 24 h post infection coverslips were placed in an electrophysiology recording chamber (~1 ml) and bathed in extracellular solution (mM): 140 NaCl, 5 KCl, 1 $MgSO_4$, 1.8 $CaCl_2$, 10 Hepes, pH 7.5 adjusted with NaOH/HCl. Composition of "high potassium" intracellular pipette solution (mM): 140 KCl, 5 NaCl, 2 $MgCl_2$, 1 Glucose, 10 Hepes, 1 BAPTA, pH 7.3 adjusted with KOH/HCl. "Low potassium" solution was prepared as described above with equimolar substitution of 130 mM KCl

with choline chloride (ChCl). Disodium ATP (2 mM) was added to all intracellular solutions to maintain cell energy supply. Solutions with different free Ca^{2+} concentrations were prepared by adding of Ca^{2+} and BAPTA at proportions calculated with Webmaxc software (Stanford University, USA). For control experiments in order to exclude the role of host cell extracellular calcium entry that may contribute to *T. gondii* egress, we used modified extracellular solution with $MgCl_2$ and $CaCl_2$ adjusted to 5 mM and 0.1 mM, respectively.

Quantification and Statistical Analysis

Statistical analysis of fluorescence images was performed using FIJI/ImageJ [64]. Briefly, images were background subtracted and normalized using an average of the first 5 frames of imaging. ΔF (F_{max}/F_{min}) represents the highest fold change over baseline in fluorescence after addition of stimuli or reagent. Figures were constructed using Prism analysis suite and error bars represent the standard error of the mean S.E.M. of three independent experiments. Significant differences were only considered if P values were < 0.05, where $*p < 0.05$; $**p < 0.01$; $***p < 0.001$; and $****p < 0.0001$. NS designates when the comparison is not statistically significant. Experiment-specific statistical information is provided in the figure legends or associated method details including trials (n), standard error of the mean SEM, and statistical test performed.

Supporting Information

S1 Fig. Impact of Host Histamine Signaling on *T. gondii*: A) Hela cells transiently expressing the red GECI RGECO were infected with *cyto*-GCaMP6f expressing parasites.; B) Stable Hela cell lines expressing jRGECO1a were infected with PV localized P30-jGCaMP7f expressing parasites; C) Hela cells infected with P30-RGECO *cyto*-GCaMP6f parasites. Under all conditions 100 μM Histamine was added at about 1 min mark and the response was recorded. Tracings to the right of each panel series show fluorescence fluctuations of single parasites (*green*) or of a delineated region of interest in the host cells (*red*) or PV (green) from 3 independent trials for each condition. Bar graphs represent quantification of the average ΔF values of three independent trials (Red, jRGECO1a or RGECO, *right axis*) (Green, GCaMP6f or jGCaMP7f, *left axis*). Dashed white outlines indicate the area used as a region of interest to analyze the fluorescence tracings. Dashed

white outlines highlight GCaMP6f-expressing parasites whose fluorescence tracings were used for analysis. Dashed Red outlines indicate the region of the host cell that was used to analyze for the RGECO or jRGECO1a channel. Numbers at the upper right of each panel indicate the time frame of the video.

S2 Fig. ΔPLP1 Mutants Lack the Second Ca^{2+} Peak During Egress: A) Egress was induced in Hela cells infected with ΔPLP1 GCaMP6f parasites using 100 μM Zaprinast; B & C) Representative fluorescence tracings of ΔPLP1 GCaMP6f after addition of 100 μM Zaprinast for egress and non-egressing parasites respectively. Notice, two peaks are visible for the parasites that were successfully able to egress and only one peak was visible for the parasites that were unable to egress.

S3 Fig. Calibration of Ca^{2+} Threshold: (A) RH tachyzoites (5×10^7) were loaded with FURA2-AM and resuspended in 2.5 mL of Ringer's Buffer supplemented with 100 μM EGTA. The cytosolic Ca^{2+} response to the addition of various concentrations of ionomycin is shown. The figure shows the average of at least 2 trials of each condition; (B) Quantification of Ionomycin Titration Curve. The first 15 seconds of the slope after addition of ionomycin was determined and averaged for at least two independent trials.

S1 Video. Carbachol Addition in GCaMP6f Infected Host Cells: Hela cells transiently expressing cytosolic localized RGECO were infected with cytosolic GCaMPf6 expressing parasites. 1 mM Carbachol was added at approximately the 1 min mark. (Fig. 1B shows still images from this video).

S2 Video. Thapsigargin Stimulation in LAR-GECO Expressing Host Cells: Hela cells transiently expressing the low affinity mitochondrial Ca^{2+} indicator LAR-GECO1.2 were infected with cytosolic GCaMP6f expressing parasite. 2 μM Thapsigargin was added at approximately the 1 min mark. (Fig. 2B shows still images from this video).

S3 Video. Two-peaks of Ca^{2+} contribute to Parasite Egress: Hela cells infected with cytosolic GCaMP6f parasites were treated with 100 μM of Zaprinast in media supplemented with 2 mM Ca^{2+}. (Fig. 3E shows still images from this video).

S4 Video. Natural Egress in Cpd 1 Synchronized Parasites: Hela cells stabling expressing cytosolic jRGECO1a infected with cytosolic GCaMP6f expressing parasites. After 24 hrs post infection 1 μM cpd1 was added. 24 hr post cpd1 addition parasite egress was imaged after cpd1 washout. (Fig. 4A shows still images from this video).

S5 Video. Whole-Cell Patch Clamp under High K^+ and High Ca^{2+} Conditions: Hela cells infected with GCaMP6f parasites were whole-cell patch clamped with a patch pipette solution comprising 140 mM K^+ and 10 μM Ca^{2+}. Note parasite egress is slow, methodical, and occurring one-by-one in comparison to detergents and ionophores. Video presented in real time. (Fig. 6B shows still images from this video).

S6 Video. Whole-Cell Patch Clamp under Low K^+ and High Ca^{2+} conditions: Hela cells infected with GCaMP6f parasites were whole-cell patch clamped with a patch pipette solution comprising 10 mM K^+, 130 mM choline chloride, and 10 μM Ca^{2+}. Again, parasites egress slower in comparison to detergents and ionophores, but more rapidly in comparison to high K^+ conditions. Parasite egress occurred in which all parasites egressed at once under these conditions. Video presented in real time. (Fig. 6C shows still images from this video).

S1 Table. Plasmids used in this work

Acknowledgements

We would like to thank Alex W. Chan and Dr. Sebastian Lourido for the protocol of natural egress using compound 1; Dr. Vern Carruthers for the ΔPLP1 mutant parasites; Dr. Diego Huet for reading the manuscript; Daniel Williamson for assisting on the egress of the ΔPLP1 mutant; Beejan Asady for technical assistance; Julie Nelson for the FAC's sorting assistance; Dr. Kandasamy for technical assistance on the use of the microscopes at the Biomedical Microscopy

Core. This work was supported by an NIH grant R01AI128356 to SNJM. SAV and EP were partially supported by fellowships (pre-doc and post-doc respectively) through a Training Grant in Tropical and Emerging Global Diseases (T32AI060546).

Authors Contributions

Conceived and designed the experiments: SAV, CAM, SNJM. Performed the experiments: SAV, CAM, ZHL, MAHT and EP. Analyzed the data: SAV, CAM and SNJM. Contributed reagents/materials/analysis tools: SAV, CAM, ZHL and SNJM. Wrote the paper: SAV and SNJM.

References

1. Black MW, Boothroyd JC. Lytic cycle of Toxoplasma gondii. Microbiol Mol Biol Rev. 2000;64(3):607-23. PubMed PMID: 10974128.
2. Blader IJ, Coleman BI, Chen CT, Gubbels MJ. Lytic Cycle of Toxoplasma gondii: 15 Years Later. Annu Rev Microbiol. 2015;69:463-85. Epub 2015/09/04. doi: 10.1146/annurev-micro-091014-104100. PubMed PMID: 26332089; PubMed Central PMCID: PMCPMC4659696.
3. Arrizabalaga G, Boothroyd JC. Role of calcium during Toxoplasma gondii invasion and egress. Int J Parasitol. 2004;34(3):361-8. PubMed PMID: 15003496.
4. Hortua Triana MA, Marquez-Nogueras KM, Vella SA, Moreno SNJ. Calcium signaling and the lytic cycle of the Apicomplexan parasite Toxoplasma gondii. Biochim Biophys Acta Mol Cell Res. 2018;1865(11 Pt B):1846-56. Epub 2019/04/18. doi: 10.1016/j.bbamcr.2018.08.004. PubMed PMID: 30992126; PubMed Central PMCID: PMCPMC6477927.
5. Clapham DE. Calcium signaling. Cell. 2007;131(6):1047-58. doi: 10.1016/j.cell.2007.11.028. PubMed PMID: 18083096.
6. Lovett JL, Sibley LD. Intracellular calcium stores in Toxoplasma gondii govern invasion of host cells. J Cell Sci. 2003;116(Pt 14):3009-16. PubMed PMID: 12783987.
7. Borges-Pereira L, Budu A, McKnight CA, Moore CA, Vella SA, Hortua Triana MA, et al. Calcium Signaling throughout the Toxoplasma gondii Lytic Cycle: A STUDY USING GENETICALLY ENCODED CALCIUM INDICATORS. J Biol Chem. 2015;290(45):26914-26. Epub 2015/09/17. doi: 10.1074/jbc.M115.652511. PubMed PMID: 26374900; PubMed Central PMCID: PMCPMC4646405.
8. Lourido S, Moreno SN. The calcium signaling toolkit of the Apicomplexan parasites Toxoplasma gondii and Plasmodium spp. Cell Calcium. 2015;57(3):186-93. Epub 2015/01/22. doi: 10.1016/j.ceca.2014.12.010. PubMed PMID: 25605521; PubMed Central PMCID: PMCPMC4428288.
9. Frenal K, Polonais V, Marq JB, Stratmann R, Limenitakis J, Soldati-Favre D. Functional dissection of the apicomplexan glideosome molecular architecture. Cell Host Microbe. 2010;8(4):343-57. Epub 2010/10/19. doi: 10.1016/j.chom.2010.09.002. PubMed PMID: 20951968.

10. Endo T, Sethi KK, Piekarski G. Toxoplasma gondii: calcium ionophore A23187-mediated exit of trophozoites from infected murine macrophages. Exp Parasitol. 1982;53(2):179-88. PubMed PMID: 6800836.
11. Kafsack BF, Pena JD, Coppens I, Ravindran S, Boothroyd JC, Carruthers VB. Rapid membrane disruption by a perforin-like protein facilitates parasite exit from host cells. Science. 2009;323(5913):530-3. Epub 2008/12/20. doi: 10.1126/science.1165740. PubMed PMID: 19095897; PubMed Central PMCID: PMCPMC2662845.
12. Schwab JC, Beckers CJ, Joiner KA. The parasitophorous vacuole membrane surrounding intracellular Toxoplasma gondii functions as a molecular sieve. Proc Natl Acad Sci U S A. 1994;91(2):509-13. PubMed PMID: 8290555.
13. Hupe DJ, Pfefferkorn ER, Behrens ND, Peters K. L-651,582 inhibition of intracellular parasitic protozoal growth correlates with host-cell directed effects. J Pharmacol Exp Ther. 1991;256(2):462-7. Epub 1991/02/01. PubMed PMID: 1993990.
14. Pingret L, Millot JM, Sharonov S, Bonhomme A, Manfait M, Pinon JM. Relationship between intracellular free calcium concentrations and the intracellular development of Toxoplasma gondii. J Histochem Cytochem. 1996;44(10):1123-9. PubMed PMID: 8813077.
15. Dana H, Mohar B, Sun Y, Narayan S, Gordus A, Hasseman JP, et al. Sensitive red protein calcium indicators for imaging neural activity. Elife. 2016;5. Epub 2016/03/25. doi: 10.7554/eLife.12727. PubMed PMID: 27011354; PubMed Central PMCID: PMCPMC4846379.
16. Zhao Y, Araki S, Wu J, Teramoto T, Chang YF, Nakano M, et al. An expanded palette of genetically encoded Ca(2)(+) indicators. Science. 2011;333(6051):1888-91. Epub 2011/09/10. doi: 10.1126/science.1208592. PubMed PMID: 21903779.
17. Dana H, Sun Y, Mohar B, Hulse BK, Kerlin AM, Hasseman JP, et al. High-performance calcium sensors for imaging activity in neuronal populations and microcompartments. Nat Methods. 2019;16(7):649-57. Epub 2019/06/19. doi: 10.1038/s41592-019-0435-6. PubMed PMID: 31209382.
18. Walker JK, Gainetdinov RR, Feldman DS, McFawn PK, Caron MG, Lefkowitz RJ, et al. G protein-coupled receptor kinase 5 regulates airway responses induced by muscarinic receptor activation. Am J Physiol Lung Cell Mol Physiol. 2004;286(2):L312-9. Epub 2003/10/21. doi: 10.1152/ajplung.00255.2003. PubMed PMID: 14565944.
19. Ockenga W, Kuhne S, Bocksberger S, Banning A, Tikkanen R. Non-neuronal functions of the m2 muscarinic acetylcholine receptor. Genes (Basel). 2013;4(2):171-97. Epub 2013/01/01. doi: 10.3390/genes4020171. PubMed PMID: 24705159; PubMed Central PMCID: PMCPMC3899973.
20. Tasaka K, Mio M, Okamoto M. Intracellular calcium release induced by histamine releasers and its inhibition by some antiallergic drugs. Ann Allergy. 1986;56(6):464-9. Epub 1986/06/01. PubMed PMID: 2424349.
21. Wu J, Prole DL, Shen Y, Lin Z, Gnanasekaran A, Liu Y, et al. Red fluorescent genetically encoded Ca2+ indicators for use in mitochondria and endoplasmic reticulum. Biochem J. 2014;464(1):13-22. Epub 2014/08/29. doi: 10.1042/BJ20140931. PubMed PMID: 25164254; PubMed Central PMCID: PMCPMC4214425.
22. Liu C, Hermann TE. Characterization of ionomycin as a calcium ionophore. The Journal of biological chemistry. 1978;253(17):5892-4. Epub 1978/09/10. PubMed PMID: 28319.

23. Berman MC. Characterisation of thapsigargin-releasable Ca(2+) from the Ca(2+)-ATPase of sarcoplasmic reticulum at limiting [Ca(2+)]. Biochim Biophys Acta. 2000;1509(1-2):42-54. Epub 2000/12/19. doi: 10.1016/s0005-2736(00)00280-7. PubMed PMID: 11118516.
24. Tepikin AV. Mitochondrial junctions with cellular organelles: Ca(2+) signalling perspective. Pflugers Arch. 2018;470(8):1181-92. Epub 2018/07/10. doi: 10.1007/s00424-018-2179-z. PubMed PMID: 29982949; PubMed Central PMCID: PMCPMC6060751.
25. Sidik SM, Hortua Triana MA, Paul AS, El Bakkouri M, Hackett CG, Tran F, et al. Using a Genetically Encoded Sensor to Identify Inhibitors of Toxoplasma gondii Ca2+ Signaling. J Biol Chem. 2016;291(18):9566-80. Epub 2016/03/05. doi: 10.1074/jbc.M115.703546. PubMed PMID: 26933036; PubMed Central PMCID: PMCPMC4850295.
26. Lourido S, Tang K, Sibley LD. Distinct signalling pathways control Toxoplasma egress and host-cell invasion. EMBO J. 2012;31(24):4524-34. Epub 2012/11/15. doi: 10.1038/emboj.2012.299. PubMed PMID: 23149386; PubMed Central PMCID: PMCPMC3545288.
27. Collins CR, Hackett F, Strath M, Penzo M, Withers-Martinez C, Baker DA, et al. Malaria parasite cGMP-dependent protein kinase regulates blood stage merozoite secretory organelle discharge and egress. PLoS Pathog. 2013;9(5):e1003344. Epub 2013/05/16. doi: 10.1371/journal.ppat.1003344. PubMed PMID: 23675297; PubMed Central PMCID: PMCPMC3649973.
28. Pace DA, McKnight CA, Liu J, Jimenez V, Moreno SN. Calcium entry in Toxoplasma gondii and its enhancing effect of invasion-linked traits. J Biol Chem. 2014;289(28):19637-47. Epub 2014/05/29. doi: 10.1074/jbc.M114.565390. PubMed PMID: 24867952; PubMed Central PMCID: PMCPMC4094074.
29. Fertig N, Blick RH, Behrends JC. Whole cell patch clamp recording performed on a planar glass chip. Biophys J. 2002;82(6):3056-62. Epub 2002/05/23. doi: 10.1016/S0006-3495(02)75646-4. PubMed PMID: 12023228; PubMed Central PMCID: PMCPMC1302093.
30. Moudy R, Manning TJ, Beckers CJ. The loss of cytoplasmic potassium upon host cell breakdown triggers egress of Toxoplasma gondii. J Biol Chem. 2001;276(44):41492-501. PubMed PMID: 11526113.
31. Bisio H, Soldati-Favre D. Signaling Cascades Governing Entry into and Exit from Host Cells by Toxoplasma gondii. Annu Rev Microbiol. 2019;73:579-99. Epub 2019/09/11. doi: 10.1146/annurev-micro-020518-120235. PubMed PMID: 31500539.
32. Nagamune K, Beatty WL, Sibley LD. Artemisinin induces calcium-dependent protein secretion in the protozoan parasite Toxoplasma gondii. Eukaryotic cell. 2007;6(11):2147-56. Epub 2007/09/04. doi: 10.1128/EC.00262-07. PubMed PMID: 17766463; PubMed Central PMCID: PMC2168421.
33. Berridge MJ. Inositol trisphosphate and calcium signalling mechanisms. Biochim Biophys Acta. 2009;1793(6):933-40. Epub 2008/11/18. doi: 10.1016/j.bbamcr.2008.10.005. PubMed PMID: 19010359.
34. Parekh AB, Putney JW, Jr. Store-operated calcium channels. Physiol Rev. 2005;85(2):757-810. Epub 2005/03/25. doi: 10.1152/physrev.00057.2003. PubMed PMID: 15788710.
35. Putney JW, Bird GS. Cytoplasmic calcium oscillations and store-operated calcium influx. J Physiol. 2008;586(13):3055-9. Epub 2008/04/05. doi: 10.1113/jphysiol.2008.153221. PubMed PMID: 18388136; PubMed Central PMCID: PMCPMC2538773.
36. Berridge MJ, Galione A. Cytosolic calcium oscillators. FASEB J. 1988;2(15):3074-82. Epub 1988/12/01. doi: 10.1096/fasebj.2.15.2847949. PubMed PMID: 2847949.

37. Wetzel DM, Chen LA, Ruiz FA, Moreno SN, Sibley LD. Calcium-mediated protein secretion potentiates motility in Toxoplasma gondii. J Cell Sci. 2004;117(Pt 24):5739-48. PubMed PMID: 15507483.
38. Lovett JL, Marchesini N, Moreno SN, Sibley LD. Toxoplasma gondii microneme secretion involves intracellular Ca(2+) release from inositol 1,4,5-triphosphate (IP(3))/ryanodine-sensitive stores. J Biol Chem. 2002;277(29):25870-6. PubMed PMID: 12011085.
39. Luo S, Vieira M, Graves J, Zhong L, Moreno SN. A plasma membrane-type Ca(2+)-ATPase co-localizes with a vacuolar H(+)-pyrophosphatase to acidocalcisomes of Toxoplasma gondii. Embo J. 2001;20(1-2):55-64. PubMed PMID: 11226155.
40. Fang J, Marchesini N, Moreno SN. A Toxoplasma gondii phosphoinositide phospholipase C (TgPI-PLC) with high affinity for phosphatidylinositol. Biochem J. 2006;394(Pt 2):417-25. Epub 2005/11/18. doi: 10.1042/BJ20051393. PubMed PMID: 16288600; PubMed Central PMCID: PMCPMC1408672.
41. Bullen HE, Jia Y, Yamaryo-Botte Y, Bisio H, Zhang O, Jemelin NK, et al. Phosphatidic Acid-Mediated Signaling Regulates Microneme Secretion in Toxoplasma. Cell Host Microbe. 2016;19(3):349-60. Epub 2016/03/11. doi: 10.1016/j.chom.2016.02.006. PubMed PMID: 26962945.
42. Moreno SN, Zhong L. Acidocalcisomes in Toxoplasma gondii tachyzoites. Biochem J. 1996;313 (Pt 2):655-9. PubMed PMID: 8573106.
43. Lanner JT, Georgiou DK, Joshi AD, Hamilton SL. Ryanodine receptors: structure, expression, molecular details, and function in calcium release. Cold Spring Harb Perspect Biol. 2010;2(11):a003996. Epub 2010/10/22. doi: 10.1101/cshperspect.a003996. PubMed PMID: 20961976; PubMed Central PMCID: PMCPMC2964179.
44. Dupont G, Combettes L, Bird GS, Putney JW. Calcium oscillations. Cold Spring Harb Perspect Biol. 2011;3(3). Epub 2011/03/23. doi: 10.1101/cshperspect.a004226. PubMed PMID: 21421924; PubMed Central PMCID: PMCPMC3039928.
45. Choi SH, Choi DH, Song KS, Shin KH, Chun BG. Zaprinast, an inhibitor of cGMP-selective phosphodiesterases, enhances the secretion of TNF-alpha and IL-1beta and the expression of iNOS and MHC class II molecules in rat microglial cells. J Neurosci Res. 2002;67(3):411-21. Epub 2002/01/29. doi: 10.1002/jnr.10102. PubMed PMID: 11813247.
46. Brown KM, Lourido S, Sibley LD. Serum Albumin Stimulates Protein Kinase G-dependent Microneme Secretion in Toxoplasma gondii. J Biol Chem. 2016;291(18):9554-65. Epub 2016/03/05. doi: 10.1074/jbc.M115.700518. PubMed PMID: 26933037; PubMed Central PMCID: PMCPMC4850294.
47. Yang L, Uboldi AD, Seizova S, Wilde ML, Coffey MJ, Katris NJ, et al. An apically located hybrid guanylate cyclase-ATPase is critical for the initiation of Ca(2+) signaling and motility in Toxoplasma gondii. J Biol Chem. 2019;294(22):8959-72. Epub 2019/04/18. doi: 10.1074/jbc.RA118.005491. PubMed PMID: 30992368; PubMed Central PMCID: PMCPMC6552420.
48. Bullen HE, Bisio H, Soldati-Favre D. The triumvirate of signaling molecules controlling Toxoplasma microneme exocytosis: Cyclic GMP, calcium, and phosphatidic acid. PLoS Pathog. 2019;15(5):e1007670. Epub 2019/05/24. doi: 10.1371/journal.ppat.1007670. PubMed PMID: 31121005; PubMed Central PMCID: PMCPMC6532924.
49. Bisio H, Lunghi M, Brochet M, Soldati-Favre D. Phosphatidic acid governs natural egress in Toxoplasma gondii via a guanylate cyclase receptor platform. Nat Microbiol. 2019;4(3):420-8. Epub 2019/02/12. doi: 10.1038/s41564-018-0339-8. PubMed PMID: 30742070.

50. Williams MJ, Alonso H, Enciso M, Egarter S, Sheiner L, Meissner M, et al. Two Essential Light Chains Regulate the MyoA Lever Arm To Promote Toxoplasma Gliding Motility. MBio. 2015;6(5):e00845-15. Epub 2015/09/17. doi: 10.1128/mBio.00845-15. PubMed PMID: 26374117; PubMed Central PMCID: PMCPMC4600101.
51. Sinai AP, Webster P, Joiner KA. Association of host cell endoplasmic reticulum and mitochondria with the Toxoplasma gondii parasitophorous vacuole membrane: a high affinity interaction. J Cell Sci. 1997;110 (Pt 17):2117-28. Epub 1997/10/08. PubMed PMID: 9378762.
52. Tinel H, Cancela JM, Mogami H, Gerasimenko JV, Gerasimenko OV, Tepikin AV, et al. Active mitochondria surrounding the pancreatic acinar granule region prevent spreading of inositol trisphosphate-evoked local cytosolic Ca(2+) signals. EMBO J. 1999;18(18):4999-5008. Epub 1999/09/16. doi: 10.1093/emboj/18.18.4999. PubMed PMID: 10487752; PubMed Central PMCID: PMCPMC1171571.
53. Pernas L, Adomako-Ankomah Y, Shastri AJ, Ewald SE, Treeck M, Boyle JP, et al. Toxoplasma effector MAF1 mediates recruitment of host mitochondria and impacts the host response. PLoS Biol. 2014;12(4):e1001845. Epub 2014/05/02. doi: 10.1371/journal.pbio.1001845. PubMed PMID: 24781109; PubMed Central PMCID: PMCPMC4004538.
54. Vines CM. Phospholipase C. Adv Exp Med Biol. 2012;740:235-54. Epub 2012/03/29. doi: 10.1007/978-94-007-2888-2_10. PubMed PMID: 22453945.
55. Roiko MS, Svezhova N, Carruthers VB. Acidification Activates Toxoplasma gondii Motility and Egress by Enhancing Protein Secretion and Cytolytic Activity. PLoS Pathog. 2014;10(11):e1004488. Epub 2014/11/07. doi: 10.1371/journal.ppat.1004488. PubMed PMID: 25375818; PubMed Central PMCID: PMCPMC4223073.
56. Arrizabalaga G, Ruiz F, Moreno S, Boothroyd JC. Ionophore-resistant mutant of Toxoplasma gondii reveals involvement of a sodium/hydrogen exchanger in calcium regulation. J Cell Biol. 2004;165(5):653-62. PubMed PMID: 15173192.
57. Barylyuk K, Koreny L, Ke H, Butterworth S, Lassadi I, Mourier T, et al. Global mapping of protein subcellular location in apicomplexans: the parasite as we've never seen it before. Access Microbiology. 2019;1:432.
58. Miranda K, Pace DA, Cintron R, Rodrigues JC, Fang J, Smith A, et al. Characterization of a novel organelle in Toxoplasma gondii with similar composition and function to the plant vacuole. Molecular microbiology. 2010;76(6):1358-75. Epub 2010/04/20. doi: 10.1111/j.1365-2958.2010.07165.x. PubMed PMID: 20398214; PubMed Central PMCID: PMC2907454.
59. Vella SA, Calixto A, Asady B, Li ZH, Moreno SN. Genetic Indicators for Calcium Signaling studies in *Toxoplasma gondii*. Methods in Molecular Biology. 2019;Toxoplasma(in press).
60. Lou YL, Guo F, Liu F, Gao FL, Zhang PQ, Niu X, et al. miR-210 activates notch signaling pathway in angiogenesis induced by cerebral ischemia. Mol Cell Biochem. 2012;370(1-2):45-51. Epub 2012/07/27. doi: 10.1007/s11010-012-1396-6. PubMed PMID: 22833359.
61. Potapenko ES, Biancardi VC, Florschutz RM, Ryu PD, Stern JE. Inhibitory-excitatory synaptic balance is shifted toward increased excitation in magnocellular neurosecretory cells of heart failure rats. J Neurophysiol. 2011;106(3):1545-57. Epub 2011/06/24. doi: 10.1152/jn.00218.2011. PubMed PMID: 21697450; PubMed Central PMCID: PMCPMC3174805.
62. Potapenko ES, Biancardi VC, Zhou Y, Stern JE. Astrocytes modulate a postsynaptic NMDA-GABAA-receptor crosstalk in hypothalamic neurosecretory neurons. J Neurosci.

2013;33(2):631-40. Epub 2013/01/11. doi: 10.1523/JNEUROSCI.3936-12.2013. PubMed PMID: 23303942; PubMed Central PMCID: PMCPMC3756658.

63. Chemin J, Monteil A, Briquaire C, Richard S, Perez-Reyes E, Nargeot J, et al. Overexpression of T-type calcium channels in HEK-293 cells increases intracellular calcium without affecting cellular proliferation. FEBS Lett. 2000;478(1-2):166-72. Epub 2000/08/03. doi: 10.1016/s0014-5793(00)01832-9. PubMed PMID: 10922490.
64. Schindelin J, Arganda-Carreras I, Frise E, Kaynig V, Longair M, Pietzsch T, et al. Fiji: an open-source platform for biological-image analysis. Nat Methods. 2012;9(7):676-82. doi: 10.1038/nmeth.2019. PubMed PMID: 22743772; PubMed Central PMCID: PMCPMC3855844.

Figure Legends

Figure 1: Ca^{2+} Host Signaling and *T. gondii* egress: A) Representative Images of Hela cells transiently expressing the red GECI RGECO that were infected with *cyto*-GCaMP6f expressing parasites. 1 mM Carbachol was added 1 min after recording started. B) Representative Images of Hela cells stably expressing jRGECO1a that were infected with PV localized P30-jGCaMP7f expressing tachyzoites. 1 mM Carbachol was added 1 min after recording started. C) Representative images of Hela cells infected with P30-RGECO *cyto*-GCaMP6f. 1 mM Carbachol was added 1 min after recording started

Tracings to the right of each panel shows fluorescence fluctuations of single parasites (*green*) or of a delineated region of interest in the host cells (*red*) or PV (green) from 3 independent trials for each condition. Bar graphs represent quantification of the average ΔF values of three independent trials (Red, jRGECO1a or RGECO, *right axis*) (*Green*, GCaMP6f or jGCaMP7f, *left axis*). Dashed white outlines indicate the area used as a region of interest for the analyzes for fluorescence changes. Dashed white outlines show GCaMP6f-expressing parasites whose fluorescence tracings were used for analysis. Dashed red outlines indicate the region of the host cell that was used to analyze the RGECO or jRGECO1a channel. Numbers at the upper right of each panel indicate the time frame of the video.

Figure 2: Threshold for Egress: A & B) Hela cells were transiently transfected with the low affinity mitochondria Ca^{2+} indicator LAR-GECO1.2 and infected with tachyzoites expressing cyto-GCaMP6f for approximately 20 h. The mitochondria surrounding each PV is labeled with the LAR-GECO1.2 (*red*). 1 μM Ionomycin (IO) and 2 μM Thapsigargin (TG) were added, respectively at 1 min and the response recorded. Dashed white outlines indicate the region of interest used for the analysis of the fluorescence changes. Dashed white outlines show GCaMP6f-expressing parasites whose fluorescence tracings were used for analysis. Dashed red outlines indicate the region of the host cell that was used to analyze for the LAR-GECO1.2 channel. Numbers at the upper right of each panel indicate the time frame of the video. C & D) Fluorescence tracings obtained after addition of IO or TG, respectively. Dashed white outlines shown in A&B indicate parasites used for analysis of GCaMP6f parasites. Dashed red outlines indicate region of LAR-GECO1.2 channel that was used for analysis. Numbers at the upper right of each panel indicate the time frame of the video. E) Comparison of Δ-Fluorescence values from each

Pharmacological stimulus. IO and Zaprinast (Zap) induce egress while TG and Histamine did not. F & G) Hela cells were infected with GCaMP6f parasites and IO was titrated down to find a concentration that did not induce egress (0.005 μM). Dashed white outlines indicate the area used as a region of interest to analyze the fluorescence changes. Numbers at the upper right of each panel indicate the time frame of the video. H & I) Fluorescence tracings of IO threshold titration of 1 μM and 0.005 μM, respectively. J) Average Δ-fluorescence values of 1, 0.1, 0.01, and 0.005 μM IO.

Figure 3: Two Peaks of Ca^{2+} Precede Egress: A & D) Hela cells infected with GCaMP6f parasites bathed in Ringer Buffer supplemented with either 2 mM Ca^{2+} (Ca^{2+} rich) or 100 μM EGTA (Ca^{2+} free media), respectively. Dashed white outlines show the region of interest for the analysis of the fluorescence changes shown in the tracings. Numbers at the upper right of each panel indicate the time frame of the video. B & E) Representative fluorescence tracings of single parasites under Zaprinast simulation in the presence and absence of extracellular Ca^{2+}, respectively. Under Ca^{2+}-free conditions (100 μM EGTA) the second peak is reduced. C) Quantification of GCaMP6f peak number preceding egress. Graph represents the summation of 3 independent experiments. F) Average time of egress comparing Zaprinast induced egress resuspended in extracellular media supplemented with either 2 mM Ca^{2+} (+) or 100 μM EGTA (-). G) Intracellular GCaMP6f parasites were exposed to the surrounding buffer under Ca^{2+} free conditions (1 mM EGTA) with a 0.01% (w/v) saponin solution in Ringer Buffer (SAP – Ca^{2+}). Dashed white outlines represent the parasites that were used in analysis. Numbers at the upper right of each panel indicate the time frame of the video. H) Representative fluorescence tracings of non-egressing parasites treated with saponin in Ca^{2+}-free conditions as shown in G. I) Intracellular GCaMP6f parasites were exposed to the surrounding buffer under Ca^{2+} rich conditions (2 mM Ca^{2+}) using a 0.01% (w/v) saponin solution in Ringer Buffer (SAP + Ca^{2+}). Dashed white outlines represent the parasites that were used for the analysis. Numbers at the upper right of each panel indicate the time frame of the video. J) Representative fluorescence tracings of egressing parasites treated with saponin in Ca^{2+}-rich conditions as shown in J.

Figure 4: Natural Egress: Intracellular GCaMP6f parasites were synchronized for natural egress with Compound 1. A) Still images of Hella cells expressing jRGECO1a infected with tachyzoites

expressing GCaMP6f and treated with 1 μM compound for 24 hours. After washout of compound 1, parasites egressed naturally within 3-5 mins; dashed regions indicate the area used as region of interest for the analysis of fluorescence changes shown in the tracings. Dashed white outlines are used to highlight GCaMP6f-expressing parasites whose fluorescence tracings were used for analysis. Dashed red outlines indicate the region of the host cell that was used to analyze for the jRGECO1a channel. Numbers at the upper right of each panel indicate the time frame of the video. B) Still images of Hella cells expressing jRGECO1a infected with ΔPLP1 tachyzoites expressing GCaMP6f and treated with 1 μM compound for 24 hours. After washout of compound 1, parasites egressed naturally within 3-5 mins; dashed regions indicate the area used as region of interest for the analysis of fluorescence changes shown in the tracings. Dashed regions are used to highlight ΔPLP1 GCaMP6f-expressing parasites whose fluorescence tracings were used for analysis. Dashed red outlines indicate the region of the host cell that was used to analyze for the jRGECO1a channel. Numbers at the upper right of each panel indicate the time frame of the video. C) Fluorescence tracings of host cell jREGO1a (red tracing) and GCaMP6f parasites (green tracings); D) Single Fluorescence tracings of host cell jREGO1a (red tracing) and GCaMP6f parasites (green tracings). Note that after compound 1 washout parasites egress still occurs with two peaks of fluorescence; E) Quantification of ΔF of jRGECO1a (red bar) and GCaMP6f (green bar) after cpd1 washout. F) Fluorescence tracings of host cell jREGO1a (red tracing) and ΔPLP1 GCaMP6f parasites (green tracings)

Figure 5: Pharmacological inhibition of Ca^{2+} influx leads to Inhibition of Egress: A) GCaMP6f infected host cells were exposed to a buffer supplemented with 2 mM Ca^{2+} containing 0.01% (w/v) saponin, and fluorescence changes were recorded. B) Fluorescence tracings of egressing parasites after addition of saponin in media supplemented with 2 mM Ca^{2+}; C) Hela cells infected with tachyzoites expressing GCaMP6f were pretreated for 5 min with 10 μM Nifedipine, a L-type Voltage Gated Calcium Channel Blocker in the presence of an extracellular buffer supplemented with 2 mM Ca^{2+} containing 0.01% (w/v) saponin and fluorescence changes were recorded. Note that parasites did not egress under these conditions; D) Fluorescence tracings of GCaMP6f parasites pretreated with Nifedipine after saponin permeabilization. E) Hela cells infected with GCaMP6f expressing tachyzoites were treated with 100 μM Zaprinast and egressed rapidly afterwards; F) Fluorescence tracings of GCaMP6f parasites treated with 100 μM Zaprinast

as indicated by the dashed outlines in E. G) Hela cells infected with GCaMP6f expressing tachyzoites were pretreated with 1 μM of compound 1 for 5 mins. After addition of 100 μM Zaprinast, parasite cytosolic Ca^{2+} slightly and briefly oscillated but no egress was evident; H) Fluorescence tracings after pretreatment with 1 μM compound 1 and stimulation of egress with 100 μM Zaprinast as indicated by the dashed white outlines in G. dashed outlines indicate the area used as a region of interest for the analysis of the fluorescence changes shown in the tracings. For A, C, E and G, the white outlines highlight the GCaMP6f-expressing parasites whose fluorescence tracings were used for analysis presented in B, D, F and H. Numbers at the upper right of each panel indicate the time frame of the video.

Figure 6: Host-Cell Patch Clamp: Hela cells infected with GCaMP6f tachyzoites were whole-cell patch-clamped and egress was monitored. A) Whole-cell patch clamp allowed for the exposure of PVs to defined Ca^{2+} concentrations by exchanging the cytosol of the host cell with the composition of the buffer inside the patch pipette; B) Representative still images of infected host cells were patch clamped under high potassium conditions (140 mM K^+) to mimic the high potassium environment of the host cytosol. Gradually increasing concentrations of free calcium were tested to see if/when egress occurred. The percentage of egressing vs non-egressing parasites is shown in the upper left-hand corner; C) Representative still images of infected hosts cells that were patched under low potassium conditions (10 mM K^+ and 130 mM Choline Chloride) and egress was monitored under the same experimental conditions as in A; D) Percentage of egressing parasites as a function of Ca^{2+} concentration. Green, 140 mM K^+, Red, 10 mM K^+ and 130 mM K^+; E) Average time of egress under high (140 mM K^+) and low potassium conditions (10 mM K^+ and 130 mM Choline Chloride). Note that under low K^+ conditions the percentage of egressing parasites increases, and parasites egress faster.

Figure 7: Model of Host Ca^{2+} Influx During Intracellular Growth. (1) A host cell Ca^{2+} signaling event triggers an increase in host cell cytosolic Ca^{2+}. Given that the PV is in equilibrium with the host cell cytosol, PV Ca^{2+} rises simultaneously. (2) The rise in PV Ca^{2+} precedes Ca^{2+} influx into the parasite via an unknown channel thus causing a rise in the cytosolic Ca^{2+} of the parasite. (3) The increased cytosolic Ca^{2+} load of the parasite eventually returns back to basal levels as Ca^{2+} is pumped into the intracellular stores (IS). (4) The parasite continues replicating

within the host cell while utilizing the Ca^{2+} influx from the host cell to maintain IS Ca^{2+} levels sufficient enough to be eventually utilized and released during egress.

Figure 1

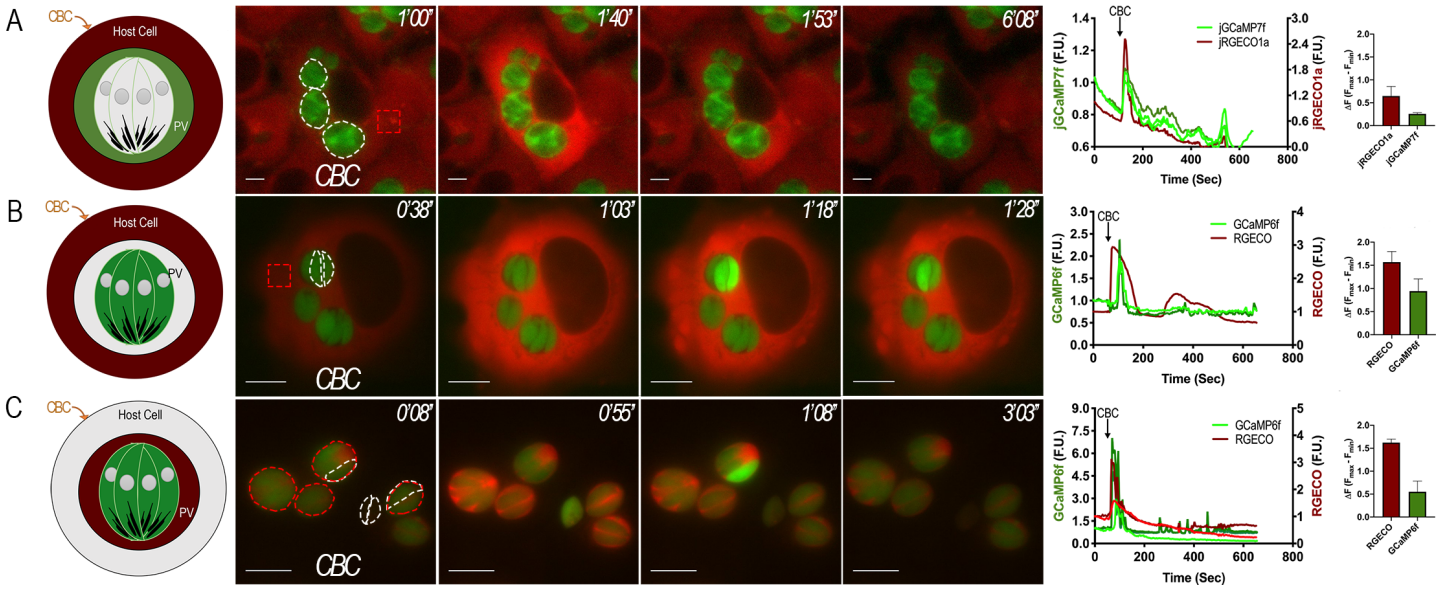
A
CBC
Host Cell
PV
1'00"
1'40'
1'53"
6'08"
CBC
jGCaMP7f
jRGECO1a
jGCaMP7f (F.U.)
jRGECO1a (F.U.)
Time (Sec)
B
0'38"
1'03'
1'18"
1'28"
GCaMP6f
RGECO
GCaMP6f (F.U.)
RGECO (F.U.)
C
0'08"
0'55'
1'08"
3'03"

Figure 2

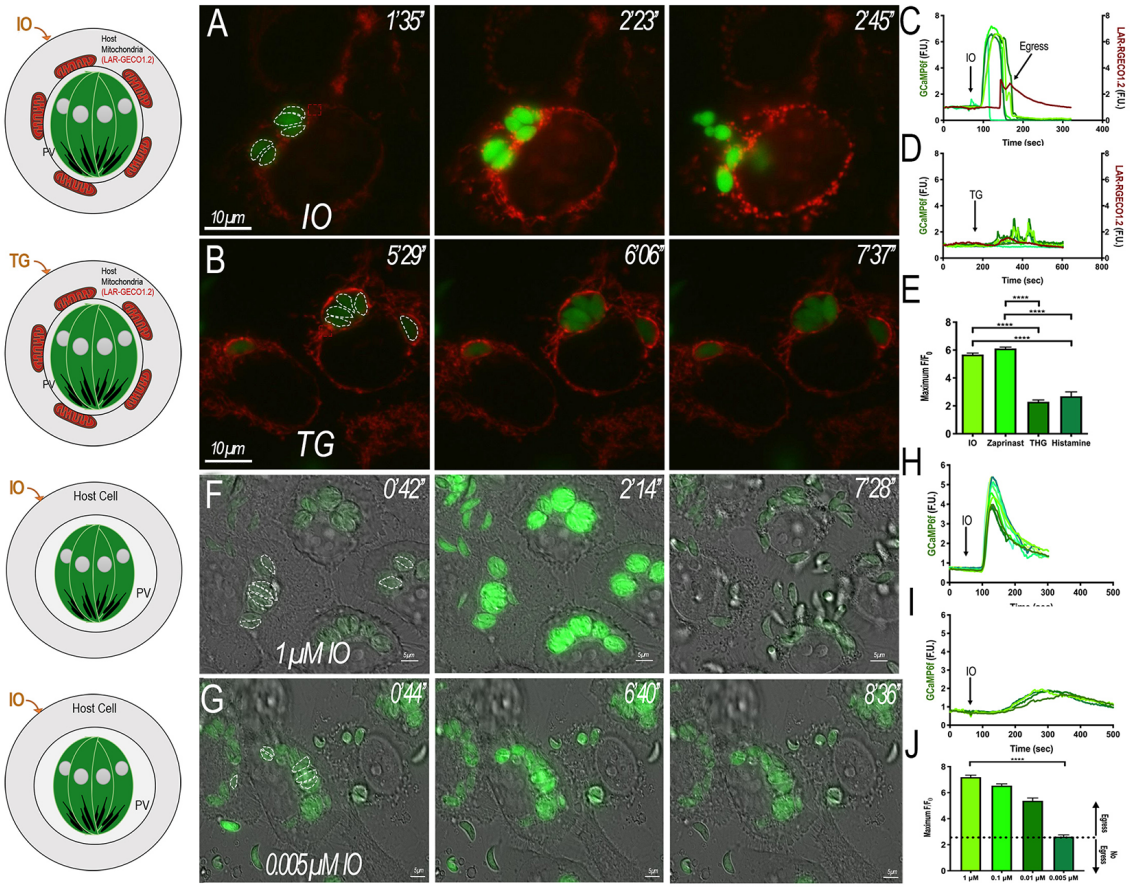
IO
Host Mitochondria (LAR-GECO1.2)
PV
TG
Host Cell
A
1'35"
2'23"
2'45"
10µm
IO
B
5'29"
6'06"
7'37"
TG
F
0'42"
2'14"
7'28"
1 µM IO
G
0'44"
6'40"
8'36"
0.005 µM IO
C
Egress
GCaMP6f (F.U.)
LAR-RGECO1.2 (F.U.)
Time (sec)
D
E
Maximum FF0
IO
Zaprinast
THG
Histamine
H
I
J
1 µM
0.1 µM
0.01 µM
0.005 µM
Egress
No Egress

Figure 3

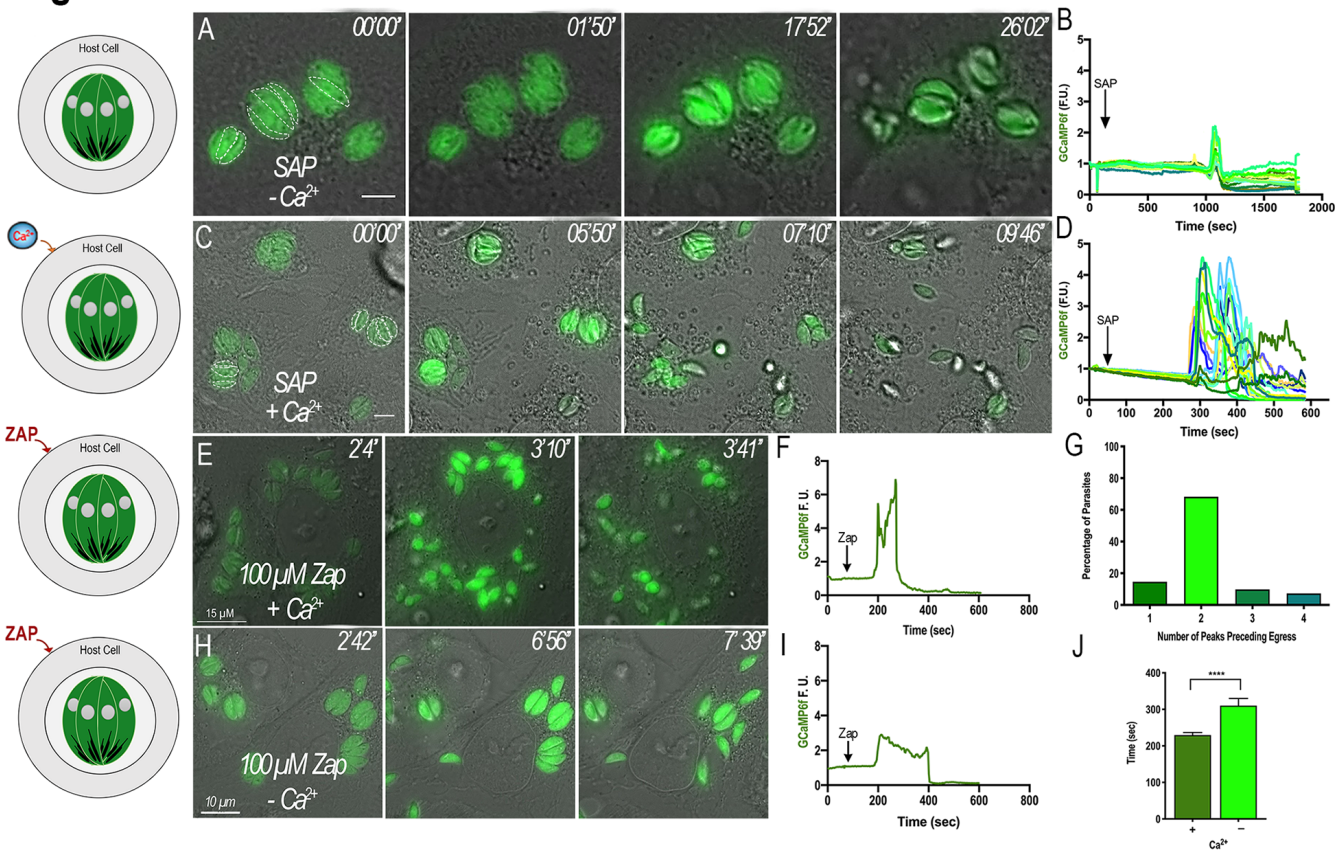
Host Cell
Host Cell
ZAP
Host Cell
ZAP
Host Cell
A
00'00"
01'50"
17'52"
26'02"
SAP
- Ca2+
B
SAP
GCaMP6f (F.U.)
Time (sec)
C
00'00"
05'50"
07'10"
09'46"
SAP
+ Ca2+
D
SAP
GCaMP6f (F.U.)
Time (sec)
E
2'4"
3'10"
3'41"
100 µM Zap
+ Ca2+
15 µM
F
Zap
GCaMP6f F. U.
Time (sec)
G
Percentage of Parasites
Number of Peaks Preceding Egress
H
2'42"
6'56"
7'39"
100 µM Zap
- Ca2+
10 µm
I
Zap
GCaMP6f F. U.
Time (sec)
J
****
Time (sec)
Ca2+

Figure 4

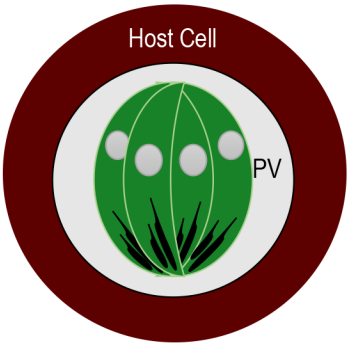
Host Cell
PV

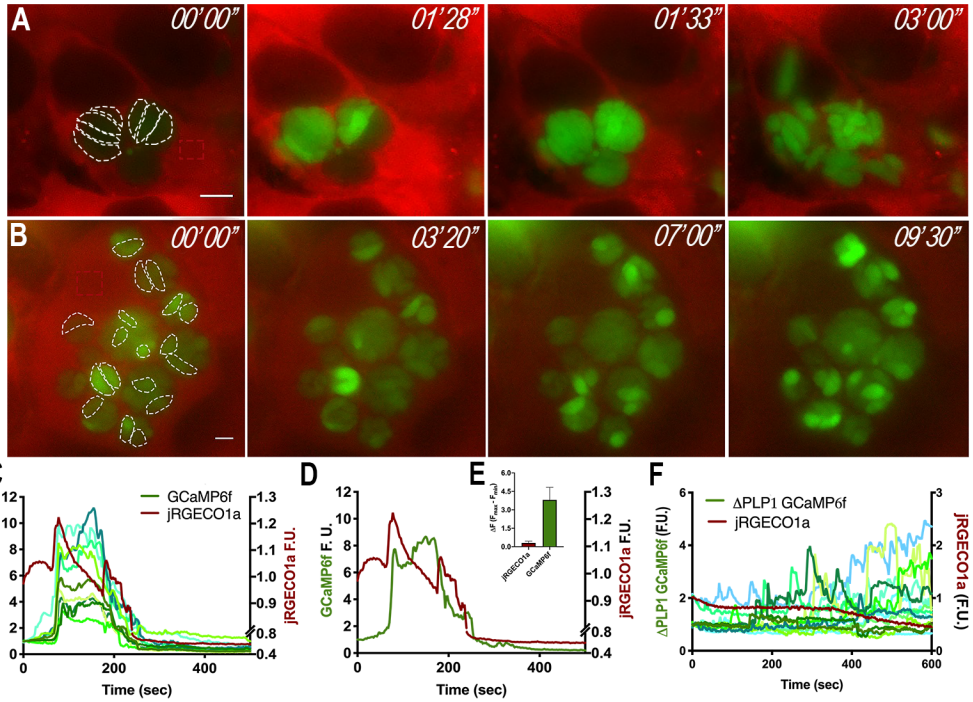
A
00'00"
01'28"
01'33"
03'00"
B
00'00"
03'20"
07'00"
09'30"
C
GCaMP6f
jRGECO1a
GCaMP6f F. U.
jRGECO1a F.U.
Time (sec)
D
GCaMP6f F. U.
jRGECO1a F.U.
Time (sec)
E
jRGECO1a
GCaMP6f
F
ΔPLP1 GCaMP6f
jRGECO1a
ΔPLP1 GCaMP6f (F.U.)
jRGECO1a (F.U.)
Time (sec)

Figure 5

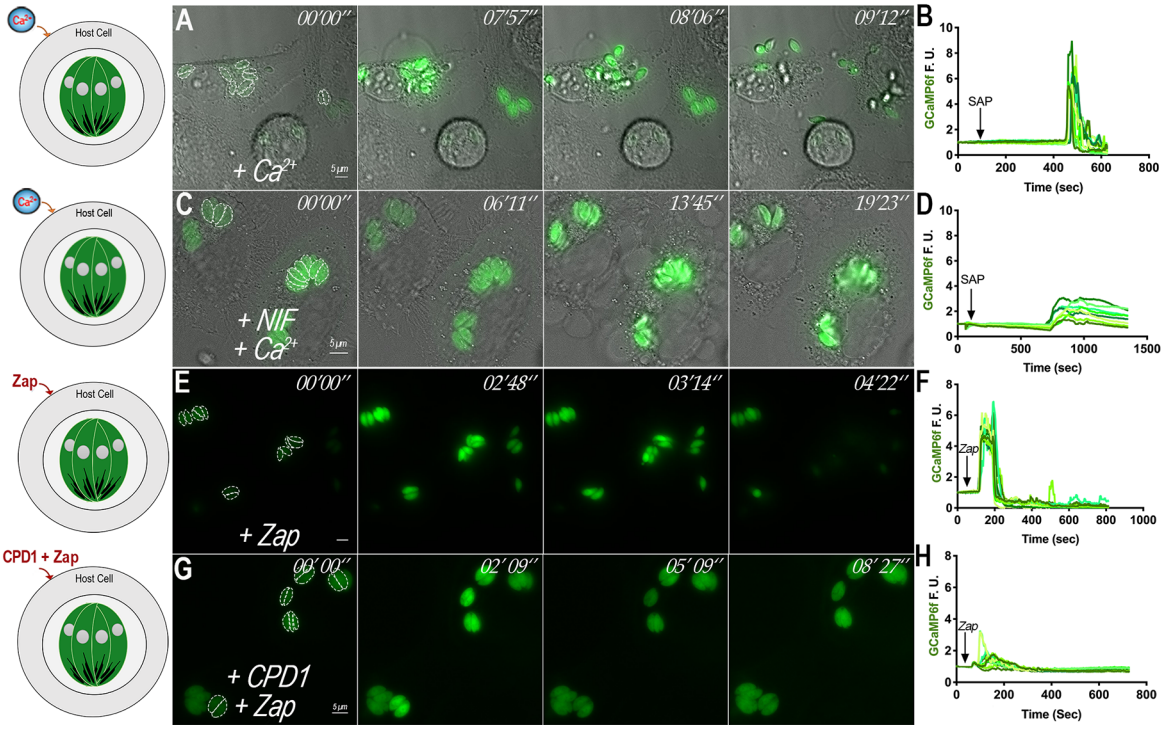
Host Cell
Zap
CPD1 + Zap
A
00′00″
07′57″
08′06″
09′12″
+ Ca2+
5 µm
B
GCaMP6f F. U.
SAP
Time (sec)
C
00′00″
06′11″
13′45″
19′23″
+ NIF
+ Ca2+
D
E
00′00″
02′48″
03′14″
04′22″
+ Zap
F
Zap
G
00′00″
02′09″
05′09″
08′27″
+ CPD1
+ Zap
H
Time (Sec)

Figure 6

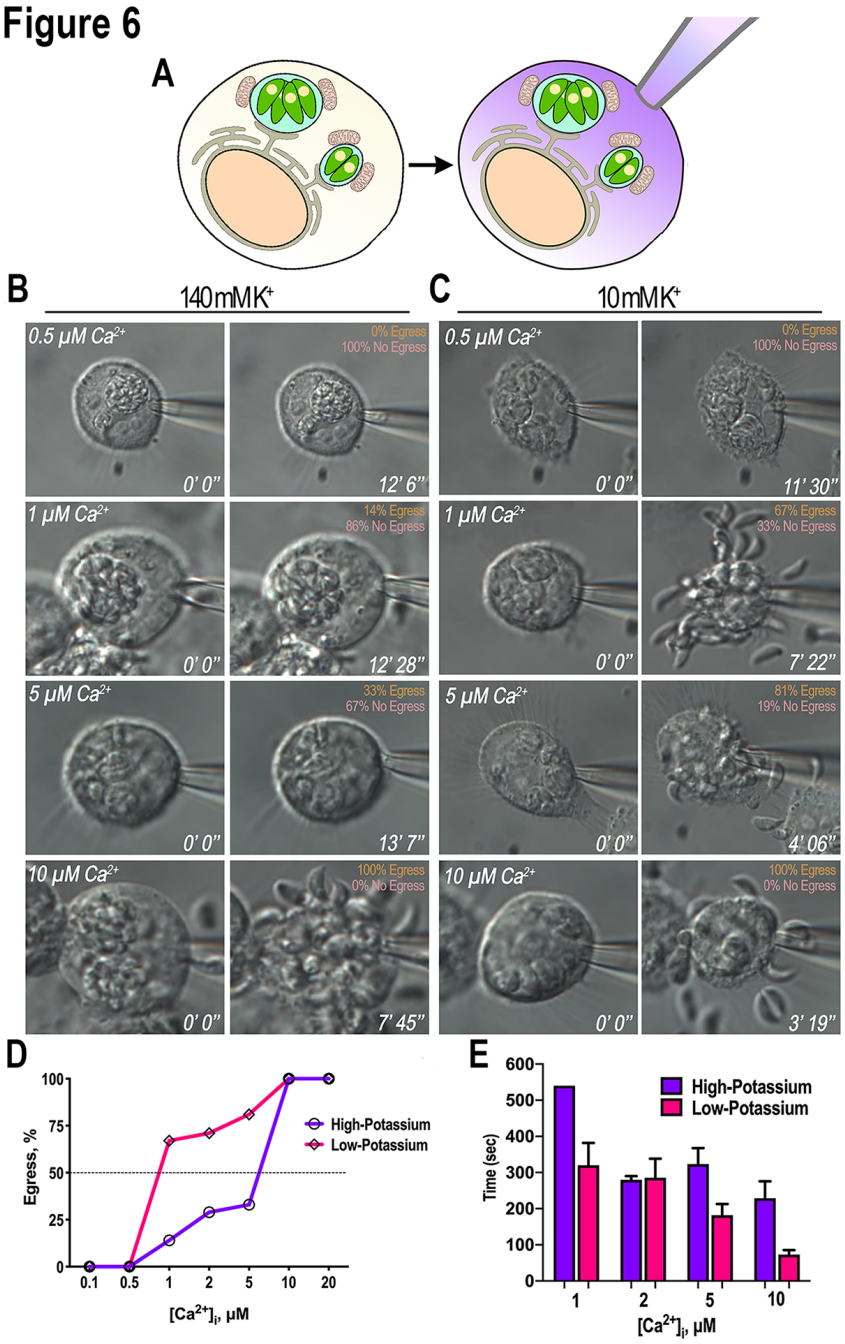
A
B
140 mM K+
C
10 mM K+
0.5 μM Ca2+
0% Egress
100% No Egress
0' 0"
12' 6"
11' 30"
1 μM Ca2+
14% Egress
86% No Egress
12' 28"
67% Egress
33% No Egress
7' 22"
5 μM Ca2+
33% Egress
67% No Egress
13' 7"
81% Egress
19% No Egress
4' 06"
10 μM Ca2+
100% Egress
0% No Egress
7' 45"
3' 19"
D
Egress, %
High-Potassium
Low-Potassium
[Ca2+]i, μM
E
Time (sec)
High-Potassium
Low-Potassium
[Ca2+]i, μM
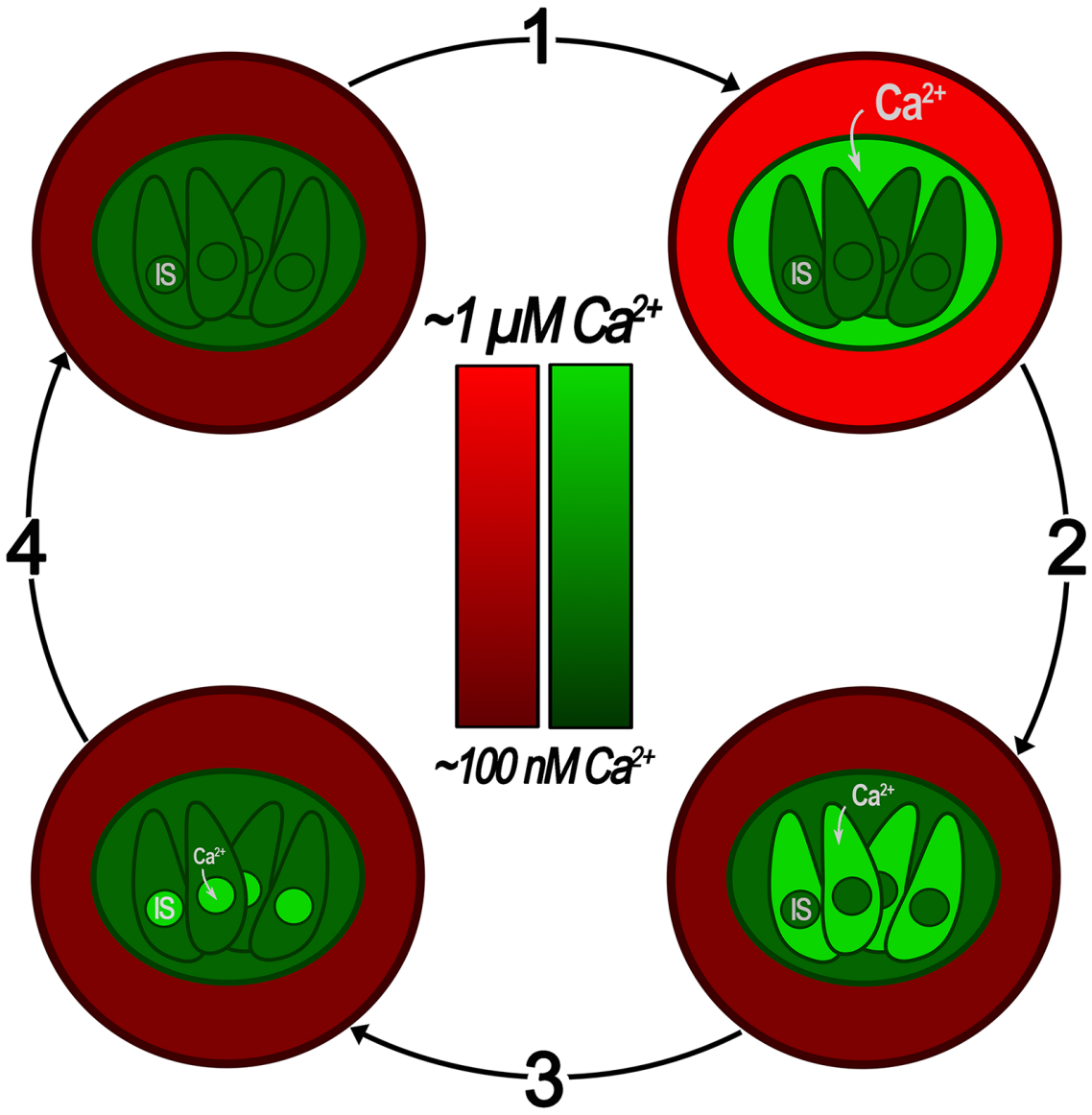
Figure 7